Spiral and Bar Pattern Time-Dependence in Galaxies

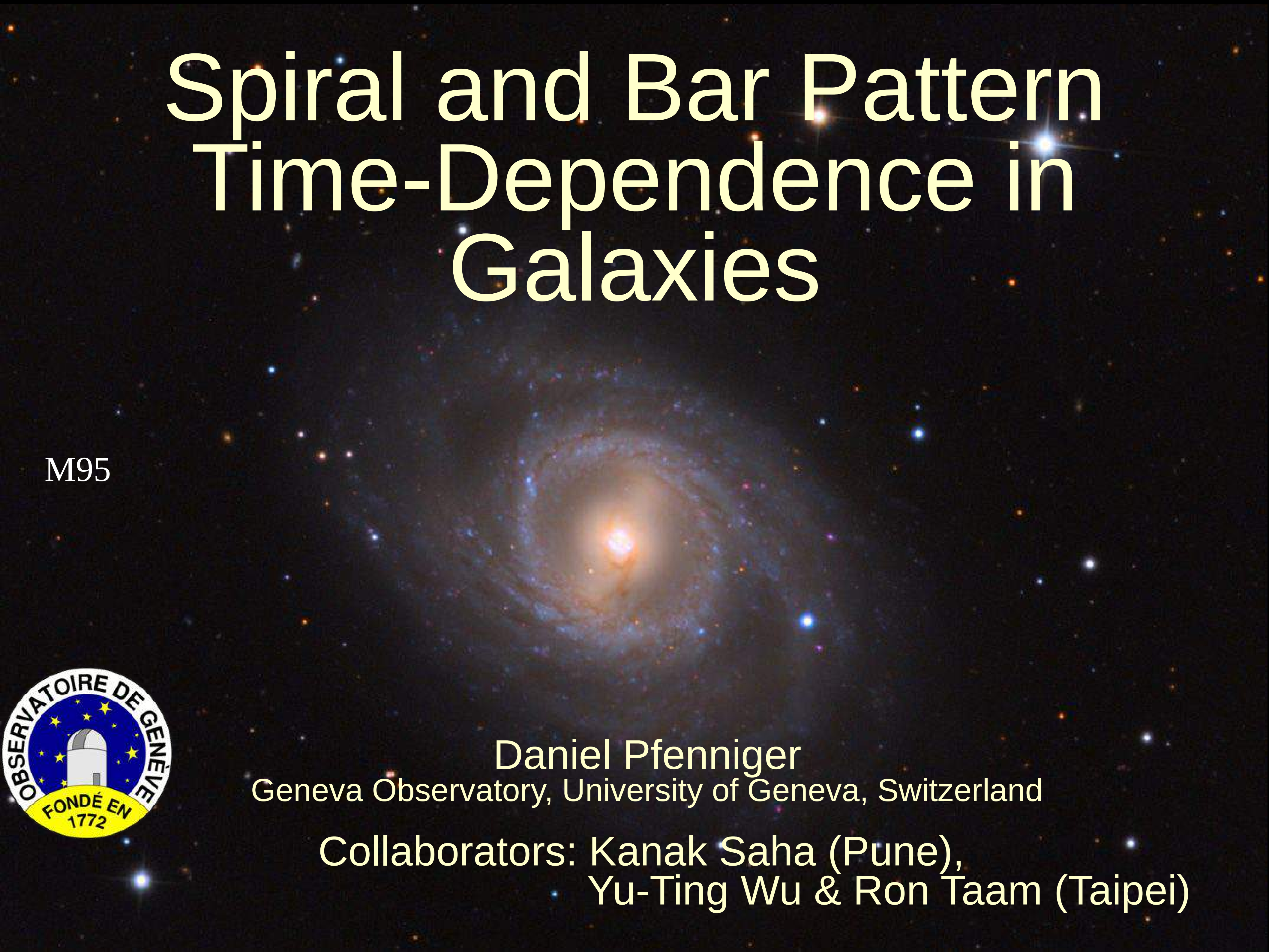

M95

Daniel Pfenniger
Geneva Observatory, University of Geneva, Switzerland

Collaborators: Kanak Saha (Pune),
Yu-Ting Wu & Ron Taam (Taipei)

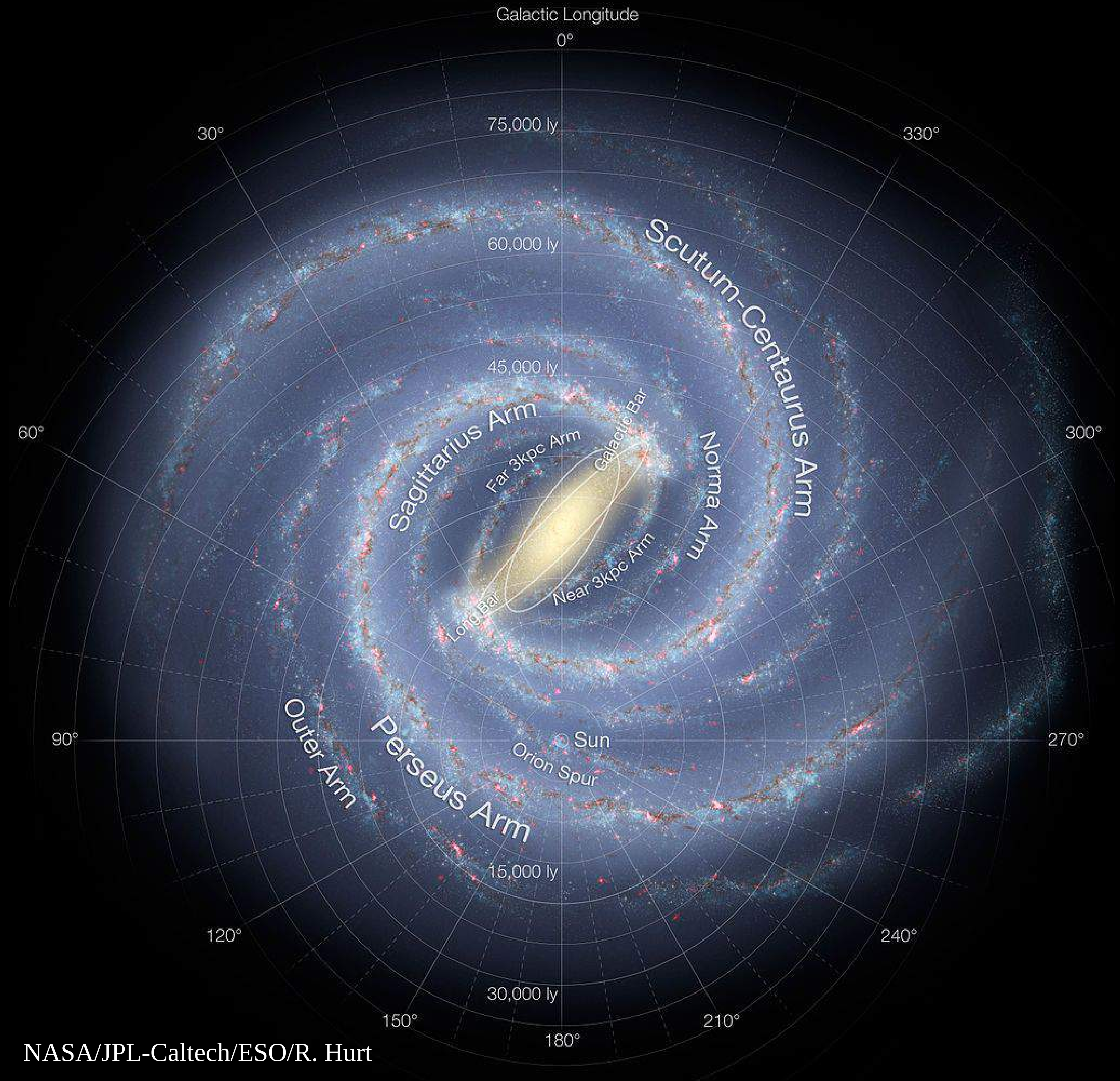

NASA/JPL-Caltech/ESO/R. Hurt

The Hubble Tuning Fork Diagram

Galaxy Morphological Classification

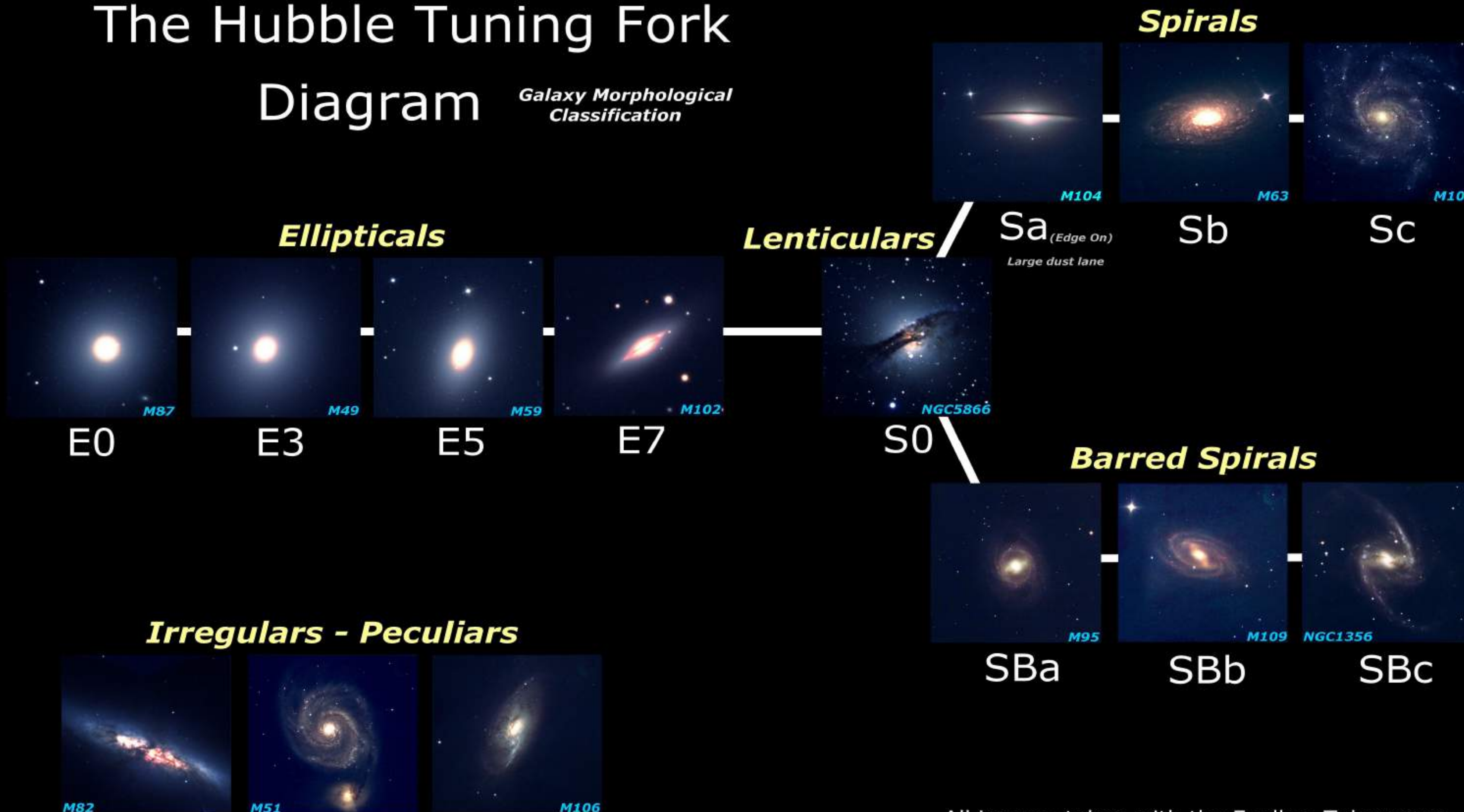

All images taken with the Faulkes Telescopes

College C.Perceret's astronomy workshop 2012

http://col21-perceret.ac-dijon.fr/col-astro

Barred galaxies, general observational facts

- At low redshifts (z<~1) about:
  - 1/3 of spirals are strongly barred
  - 1/3 of spirals are weakly barred
- But: so-classified non-barred (“normal”) galaxies include edge-on or dusty galaxies for which a stellar bar is difficult to detect
- Bars are fast rotating stellar systems
- Bars are associated with features like:
  - Nuclear, inner/outer rings, lenses
  - Boxy and peanut-shaped bulges
  - Wide open pair of spiral arms

- By now the Milky Way has been well established as barred (~ 1990-2005) with a boxy-peanut bar/bulge

Barred galaxies, general observational facts

- In a disk-bulge profile decomposition the bar length is typically ~ 2 times the bulge size
- Bars extend over the rising (linear) part of the rotation curve <=> scale

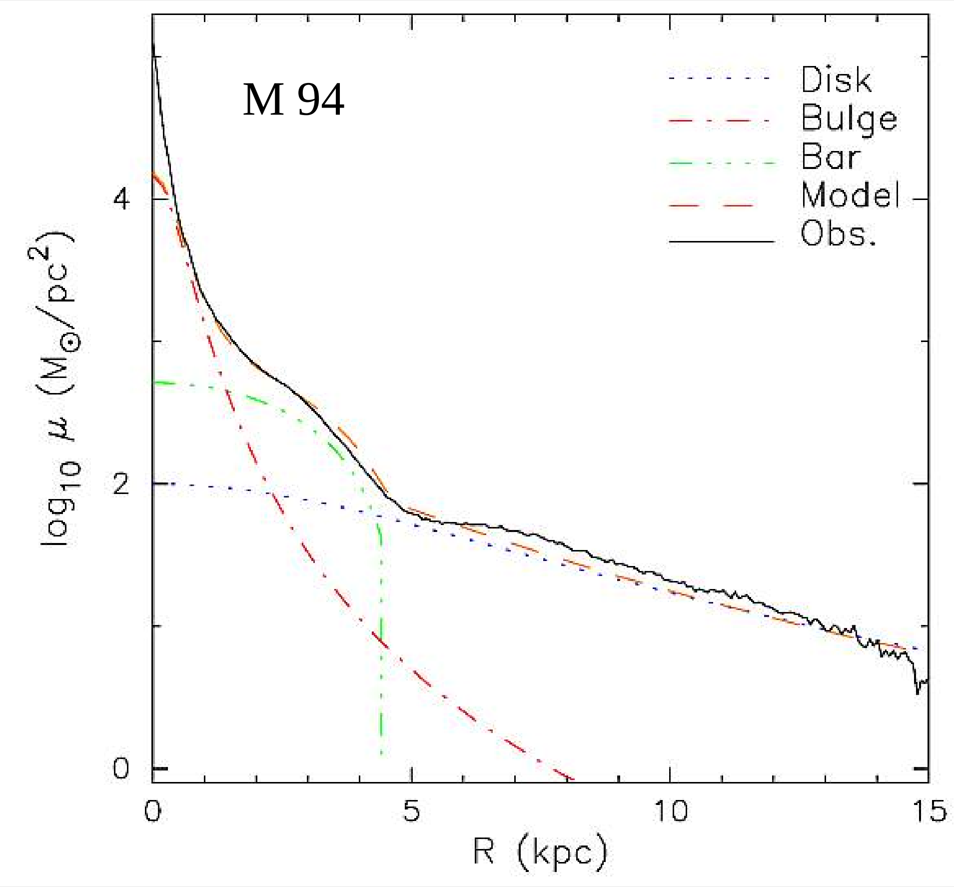

Trujillo et al . 09

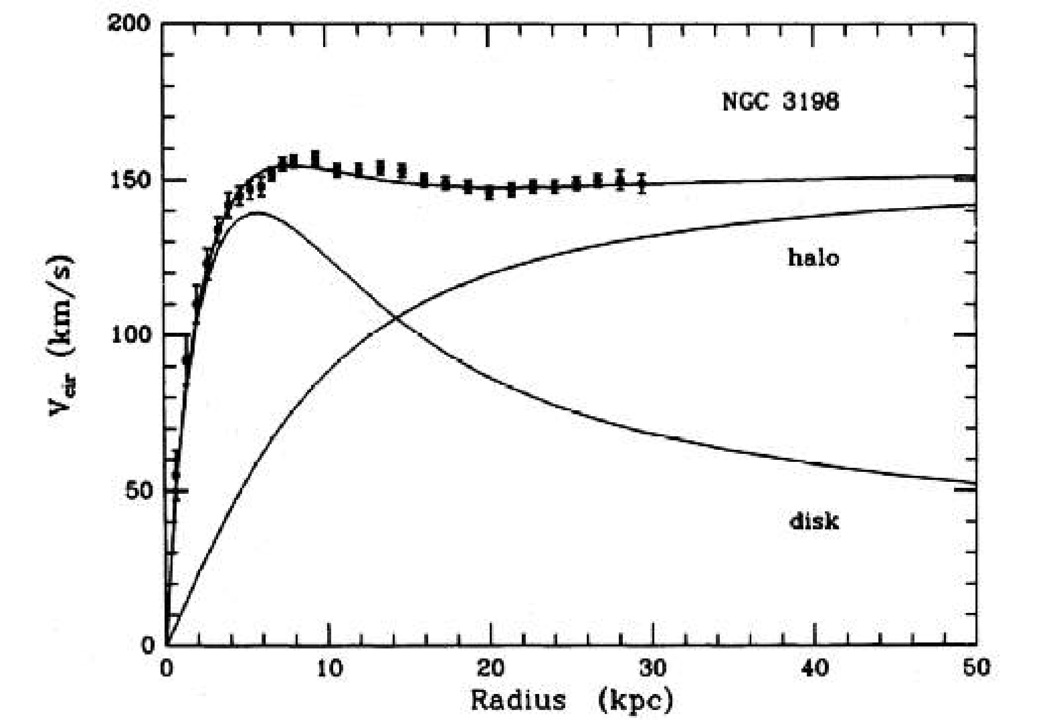

Barred galaxies, general theoretical facts

- In N-body models bars extend over the rising (linear) part of the initial rotation curve
- Bars are fast, long-lived rotating density waves, the corotation radius is slightly larger than the bar long axis
- Bars are robust to perturbations
- Spiral and bar patterns typically rotate at different speeds
  => no strict integral of motion
  => some time-dependence in
  potential unavoidable
- Nested bar(s) within a main bar rotating faster than the main bar
  => modulated time-dependence

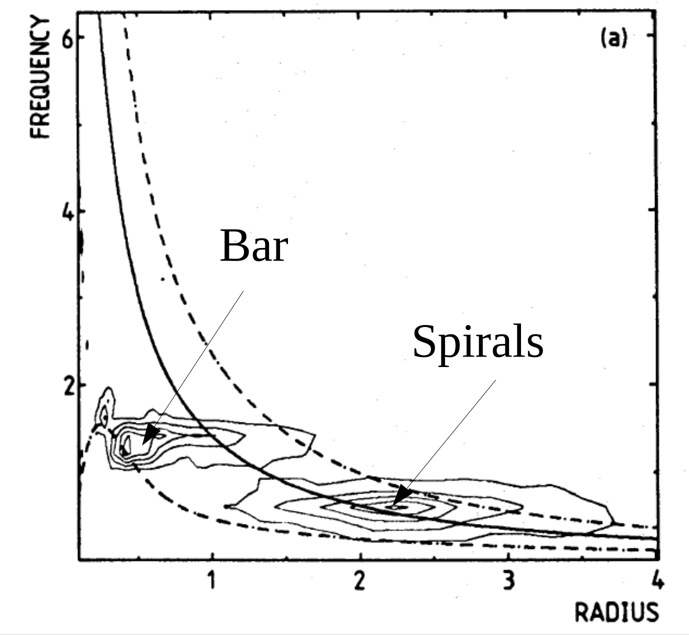

Sparke & Sellwood 87

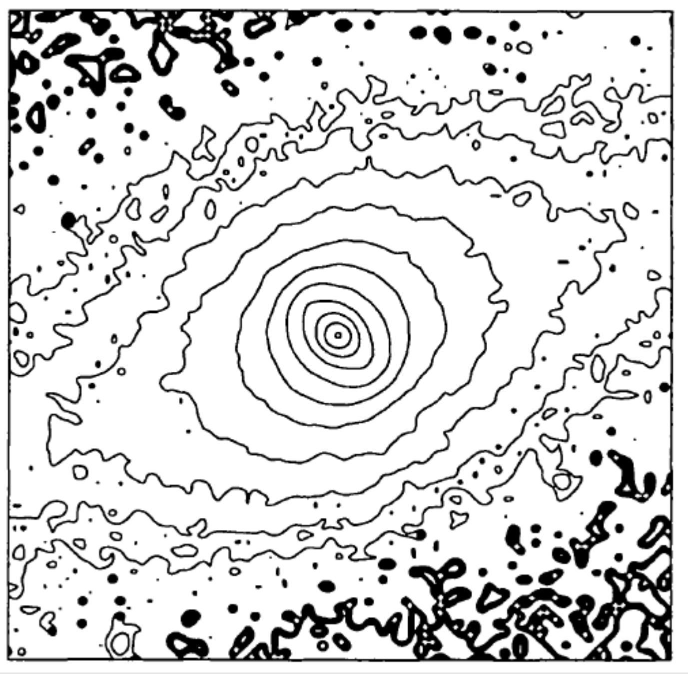
Friedli 96

Phase space geometry in steadily rotating potentials

Hamiltonian for coordinates rotating about the rotation frequency vector $\vec{\Omega}$:

$$\begin{aligned} H &= \frac{\vec{p}^{\,2}}{2} + \Phi(\vec{x},t) - \vec{\Omega}\cdot(\vec{x}\wedge\vec{p}) \\ &= \frac{\dot{\vec{x}}^{2}}{2} + \Phi(\vec{x},t) - \frac{1}{2}(\vec{\Omega}\wedge\vec{x})^2 \\ &= E - \vec{\Omega}\cdot\vec{L} \end{aligned}$$

$$\vec{p} = \dot{\vec{x}} - \vec{\Omega}\wedge\vec{x}$$

If the potential Φ is time-independent in the rotating frame, H is a global integral of motion (Jacobi integral).

In axisymmetric and steady potentials, E and L are distinct global integrals.

Phase space geometry in steadily rotating potentials

Effective potential

$$\Phi_{\text{eff}}(\vec{x}) = \Phi(\vec{x}) - \frac{1}{2}(\vec{\Omega} \wedge \vec{x})^2$$

at z=0 in a barred galaxy model

The rim of the crater (corotation) separates the bar region from the disk

Extrema = Lagrange points

The first order dynamics of barred galaxies is determined by the properties of the <u>corotation region,</u>

a gate between the bar and outer disk

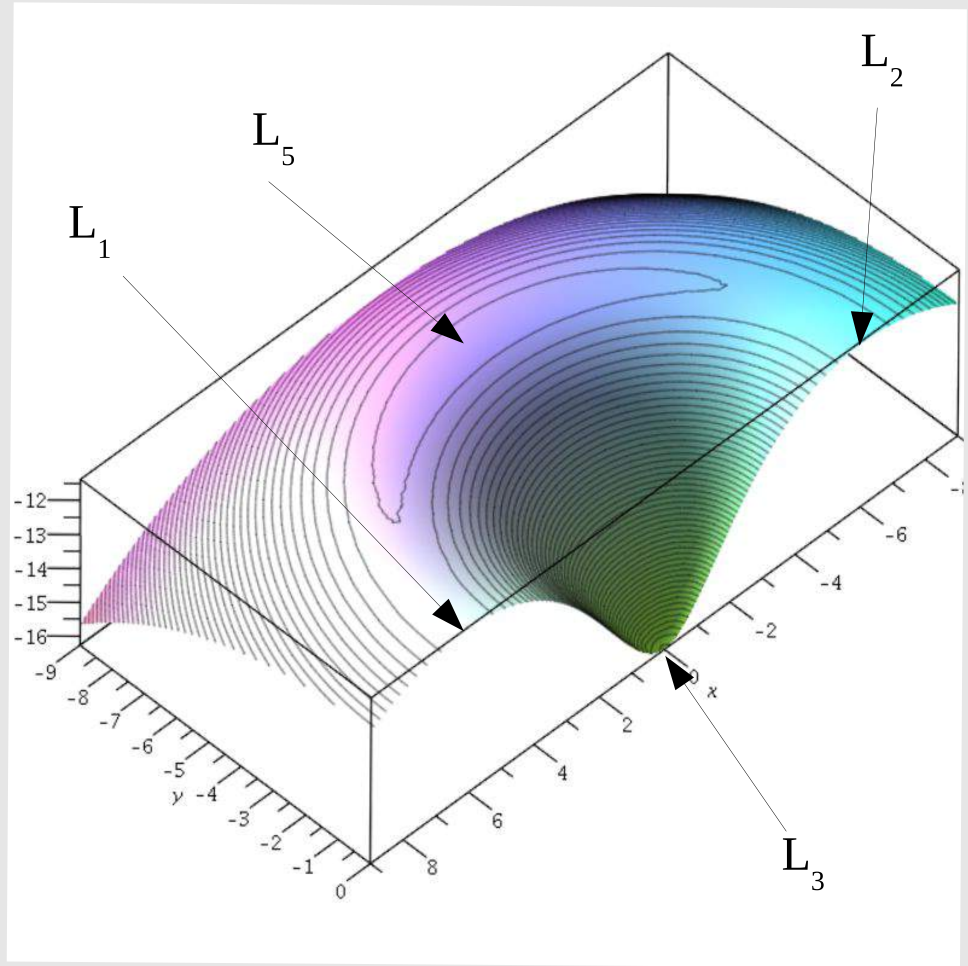

Periodic orbit families in barred galaxies

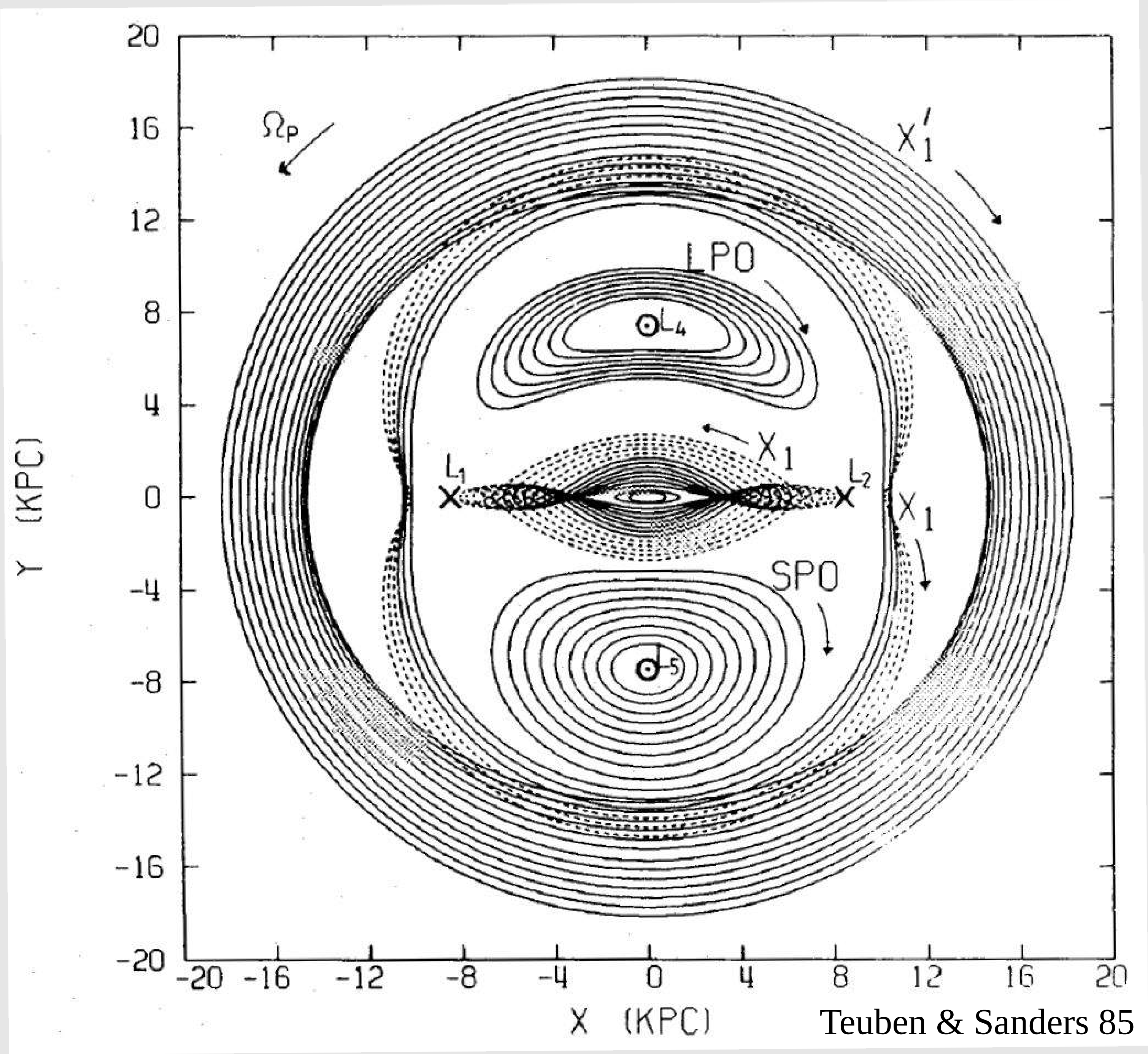

Teuben & Sanders 85

Time-dependence through bar-spiral interactions

- Time-dependence of the potential due to different bar and outer spiral pattern speeds
(Sellwood 85, Sparke & Sellwood 87, ...)
- The bar torques the spiral arms and vice-versa
  - The corotation region is reciprocally torqued by both patterns with similar strengths
  - Do Lagrange's point actually exist?

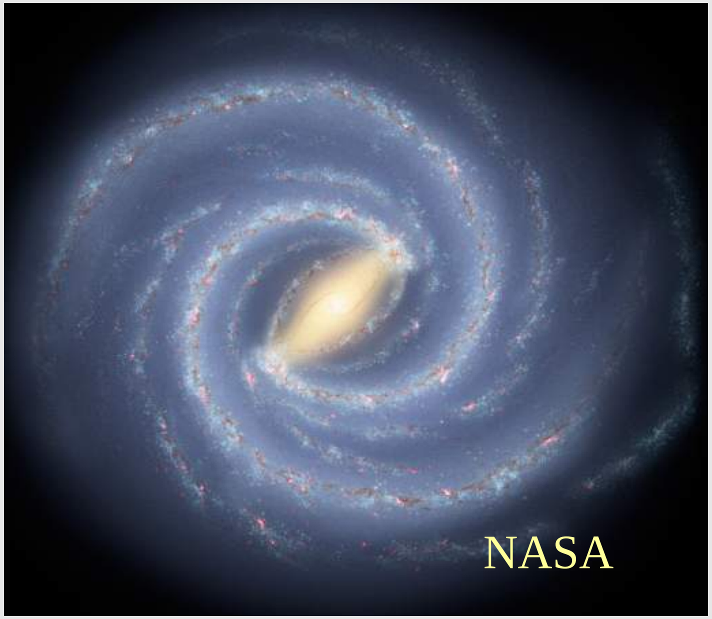

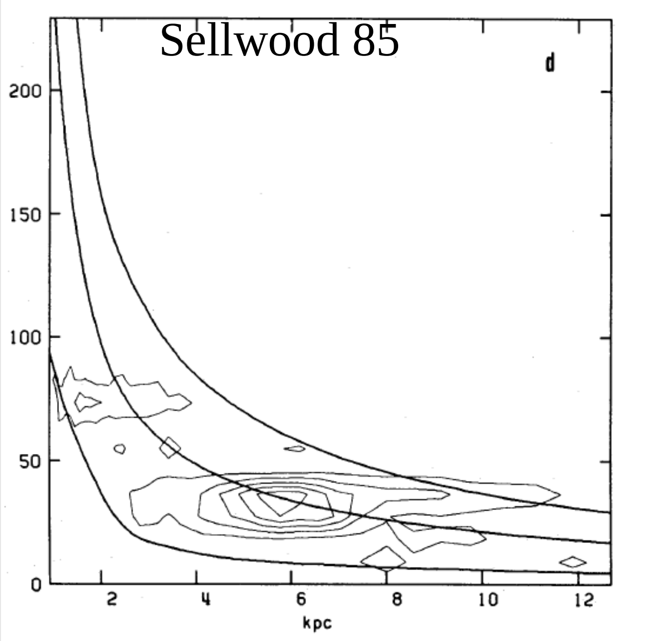

Motivations

- MW has a strong 8 kpc long bar and spiral arms, rotating presumably at distinct rotation frequencies
  - global uniformly rotating potential not realistic
- Modeling dynamics in the MW with actions and hoping to constraint the contribution of DM to the gravitational potential requires to determine
  1) the known baryonic distribution
  2) in which rotating frame dyn- amics is at most time-invariant.
- The local pattern speed parameter Ω appears as essential for any action based dynamical modeling.

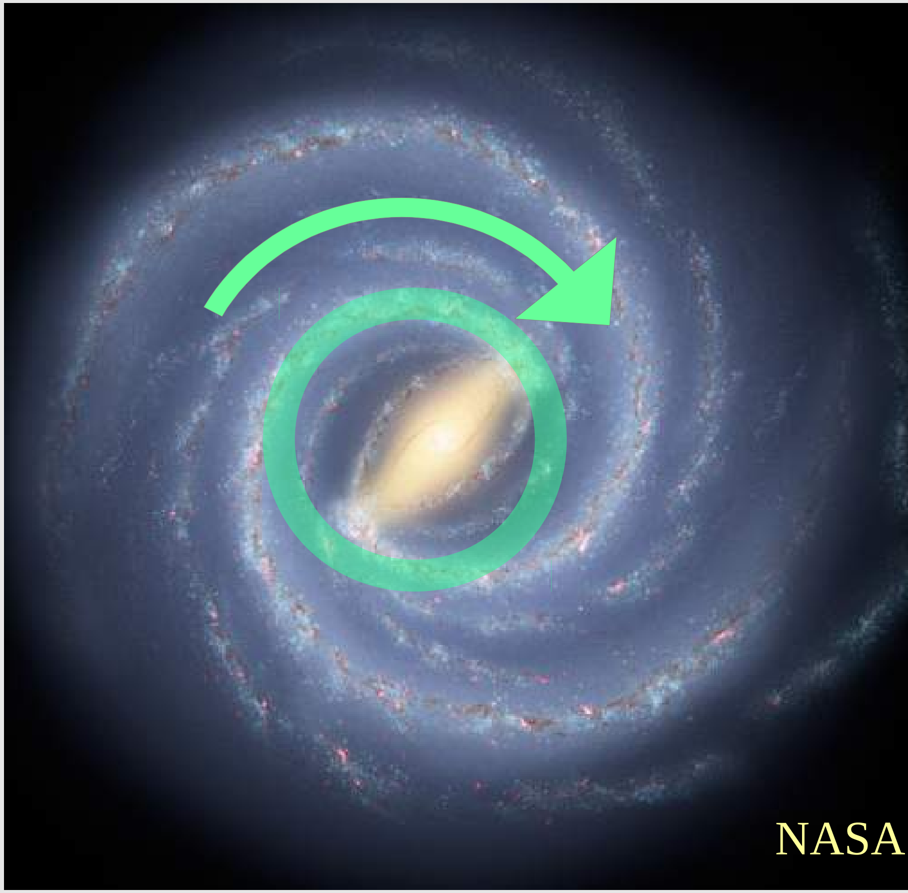

Motivations

- Gaia and other surveys will soon provide full 6D coordinates of millions of stars, an instantaneous snapshot of a subsample of the MW stars.
- Dust extinction and non-uniform sampling errors introduce severe spatial bias, however.
- Can we determine pattern frequencies from such spatially biased data sets?

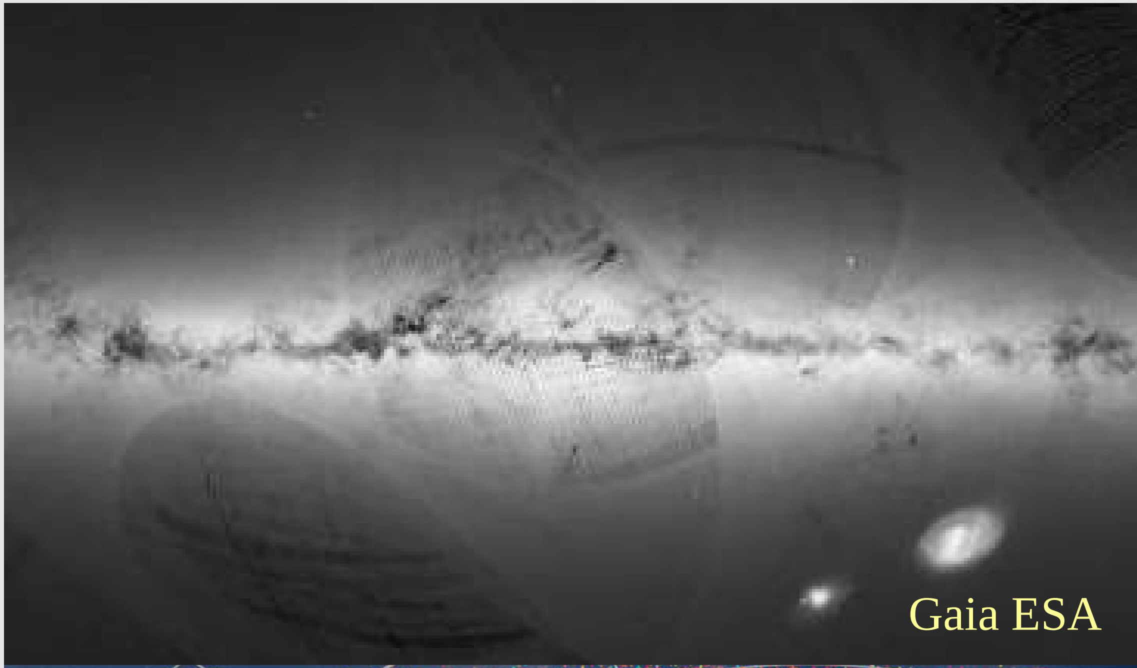

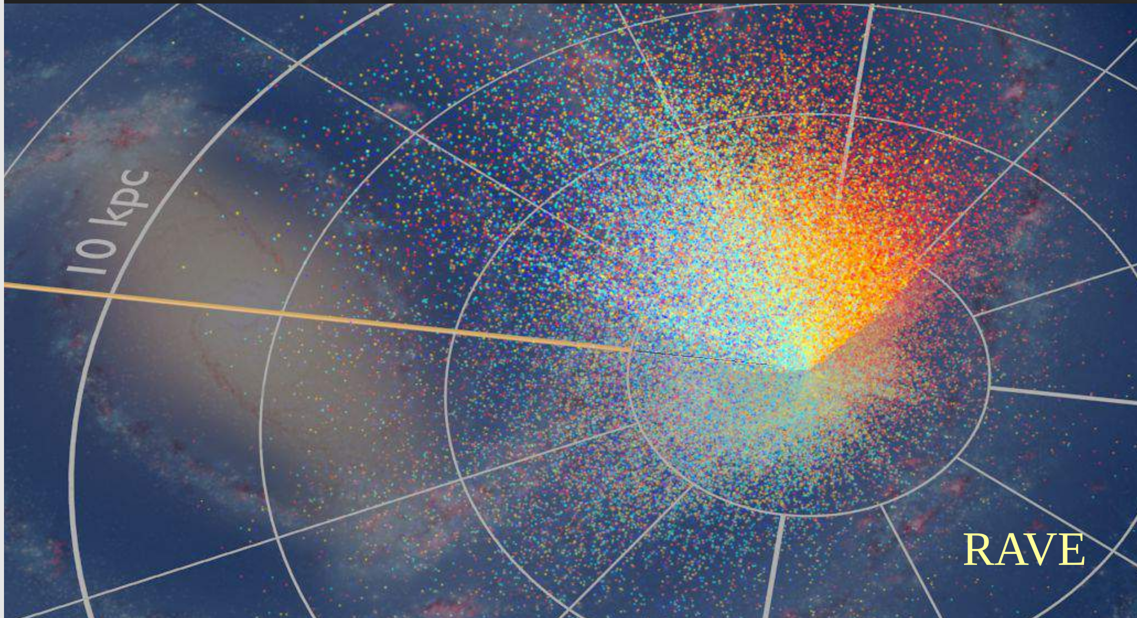

Motivations

- N-body simulations provide all the information we need, so can be used to better understand the dynamics of self-gravitating disks including multiple patterns.
- The current popular methods using time Fourier analysis (spectrograms) are unable to probe instantaneous pattern speeds and their variations.
- New methods to find instantaneous local or regional estimates of pattern speeds and accelerations are therefore required.

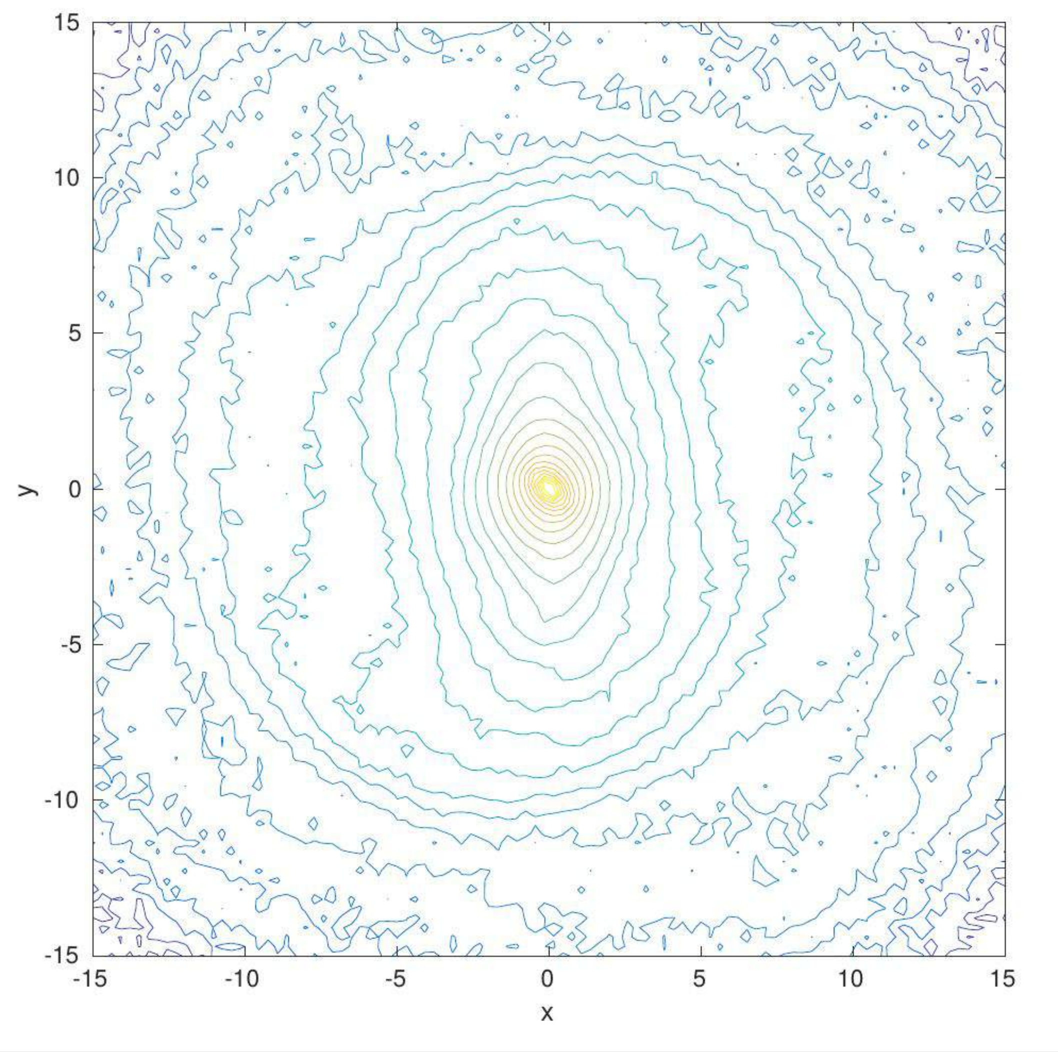


NGC 2217

Pattern speeds in galaxies

Work in progress (P, Wu & Saha)

Pattern and pattern speed popular methods

- Angular and time Fourier transforms in N-body models (2D) (Sellwood 85, Athanassoula, ...)
  => time-average pattern frequencies of rings
- Continuity equation and integration in observations and models (2D) (Tremaine Weinberg 1984, ...)
  => instantaneous pattern speed averaged over the full disk

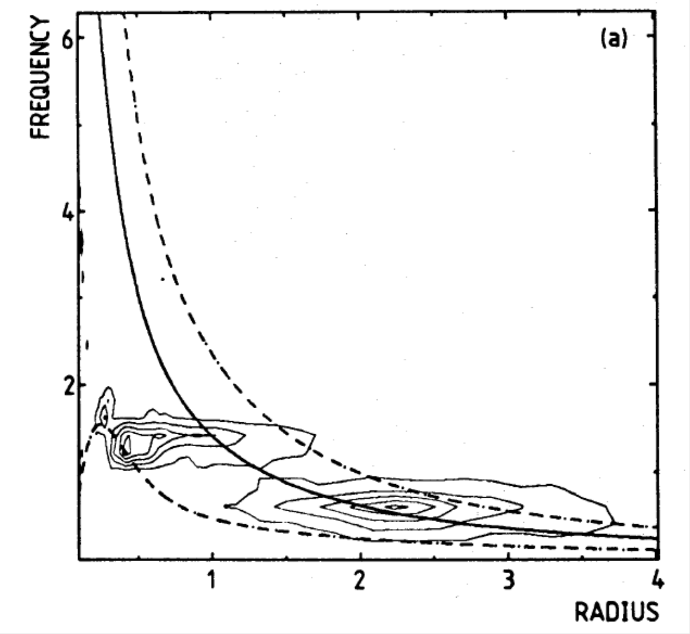

Sparke & Sellwood 87

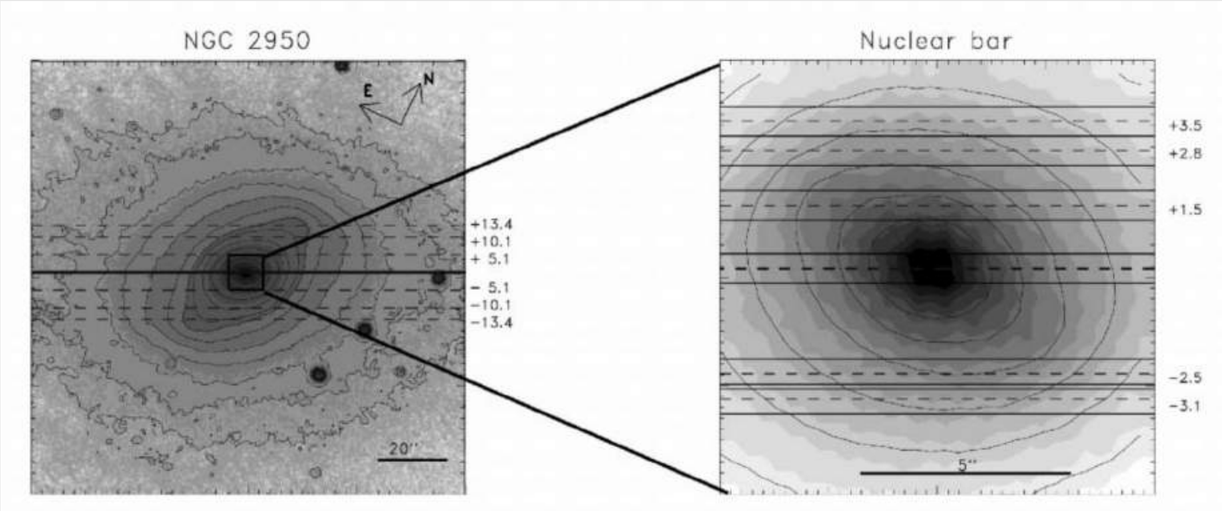

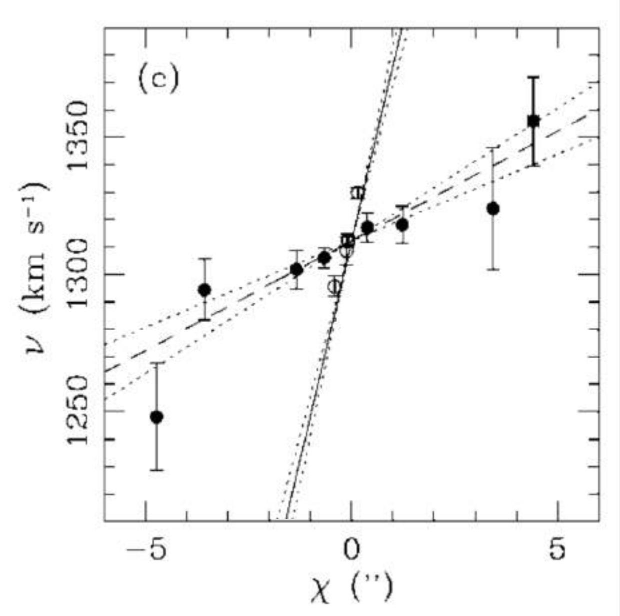

Pattern

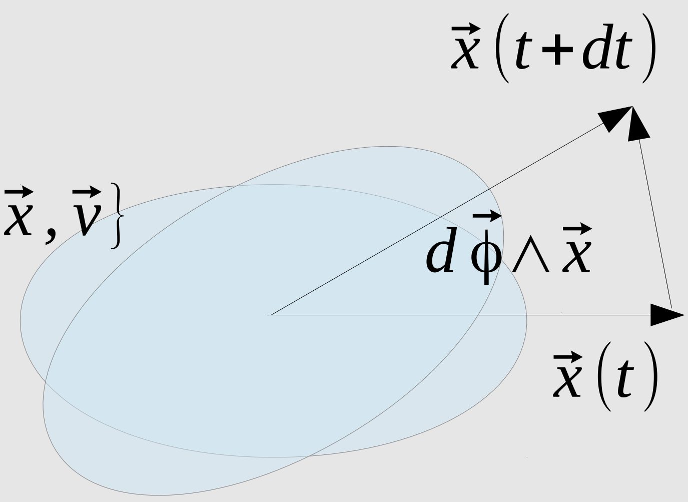

- A pattern is a function *f* of the coordinates $\{\vec{x},\vec{v}\}$ which after a time interval dt is identical to the initial function translated by $\{\vec{dx},\vec{dv}\}$ and rotated by $d\vec{\phi}$ around the center of mass.

$$\boxed{f(t+dt,\vec{x},\vec{v})=f(t,\vec{x}+\vec{dx}+\vec{d\phi}\wedge\vec{x},\vec{v}+\vec{dv}+\vec{d\phi}\wedge\vec{v})}$$

- By choosing a reference frame in the centre of mass the translation $\{\vec{dx},\vec{dv}\}$ can be removed.
- The pattern speed vector is $\vec{\Omega}=d\vec{\phi}/dt$
- Expanding to first order we get a linear equation for $\vec{\Omega}$

$$\boxed{\begin{aligned}\partial_{\vec{x}}f\cdot(\vec{\Omega}\wedge\vec{x})+\partial_{\vec{v}}f\cdot(\vec{\Omega}\wedge\vec{v}) &= \\ (\vec{x}\wedge\partial_{\vec{x}}f+\vec{v}\wedge\partial_{\vec{v}}f)\cdot\vec{\Omega} &= \partial_t f\end{aligned}}$$

Pattern speed

- If f follows a continuity equation (e.g. Boltzmann's equ.) we get a linear equation requiring to know only the phase space gradient of f

$$\boxed{\left(\vec{x}\wedge\partial_{\vec{x}}f+\vec{v}\wedge\partial_{\vec{v}}f\right)\cdot\vec{\Omega} \;=\; -\vec{v}\cdot\partial_{\vec{x}}f-\vec{a}\cdot\partial_{\vec{v}}f}$$

- This is the extension of the Tremaine-Weinberg (1984) equation to phase space and for a 3D vector $\vec{\Omega}$
- Using n>3 independent data points we get a linear system solvable by least-squares type minimization (or convex programming)

$$\begin{pmatrix} \boldsymbol{x}_1\wedge\partial_{\boldsymbol{x}}f_1+\boldsymbol{v}_1\wedge\partial_{\boldsymbol{v}}f_1 \\ \boldsymbol{x}_2\wedge\partial_{\boldsymbol{x}}f_2+\boldsymbol{v}_2\wedge\partial_{\boldsymbol{v}}f_2 \\ \vdots \\ \boldsymbol{x}_n\wedge\partial_{\boldsymbol{x}}f_n+\boldsymbol{v}_n\wedge\partial_{\boldsymbol{v}}f_n \end{pmatrix}\boldsymbol{\Omega}\approx-\begin{pmatrix} \boldsymbol{v}_1\cdot\partial_{\boldsymbol{x}}f_1+\boldsymbol{a}_1\cdot\partial_{\boldsymbol{v}}f_1 \\ \boldsymbol{v}_2\cdot\partial_{\boldsymbol{x}}f_2+\boldsymbol{a}_2\cdot\partial_{\boldsymbol{v}}f_2 \\ \vdots \\ \boldsymbol{v}_n\cdot\partial_{\boldsymbol{x}}f_n+\boldsymbol{a}_n\cdot\partial_{\boldsymbol{v}}f_n \end{pmatrix}$$

n x 3 matrix n x 1 vector

Local and regional 3D TW method

- If *f* is actually the density ρ(x,t) of a conserved population one obtains

$$\begin{pmatrix} \boldsymbol{x}_1 \wedge \partial_x \rho(\boldsymbol{x}_1) \\ \boldsymbol{x}_2 \wedge \partial_x \rho(\boldsymbol{x}_2) \\ \vdots \\ \boldsymbol{x}_n \wedge \partial_x \rho(\boldsymbol{x}_n) \end{pmatrix} \boldsymbol{\Omega}_{\mathrm{RTW}} \approx - \begin{pmatrix} \partial_x \cdot (\rho(\boldsymbol{x}_1)\, \bar{\boldsymbol{v}}(\boldsymbol{x}_1)) \\ \partial_x \cdot (\rho(\boldsymbol{x}_2)\, \bar{\boldsymbol{v}}(\boldsymbol{x}_2)) \\ \vdots \\ \partial_x \cdot (\rho(\boldsymbol{x}_n)\, \bar{\boldsymbol{v}}(\boldsymbol{x}_n)) \end{pmatrix}$$

- It is preferable to solve directly this norm minimization problem. The lines with small lhs (along the bar symmetry axes for example) add only noise and can be discarded.
- The density and mass flux gradients require complete samples in the regions where they are evaluated.

Jacobi constant 3D method

- If *f* is actually the potential Φ(x,t) one gets a linear system

$$\begin{pmatrix} \boldsymbol{x}_1 \wedge \boldsymbol{a}_1 \\ \boldsymbol{x}_2 \wedge \boldsymbol{a}_2 \\ \vdots \\ \boldsymbol{x}_n \wedge \boldsymbol{a}_n \end{pmatrix} \boldsymbol{\Omega} \approx \begin{pmatrix} \boldsymbol{v}_1 \cdot \boldsymbol{a}_1 + \dot{\Phi}(\boldsymbol{x}_1) \\ \boldsymbol{v}_2 \cdot \boldsymbol{a}_2 + \dot{\Phi}(\boldsymbol{x}_2) \\ \vdots \\ \boldsymbol{v}_n \cdot \boldsymbol{a}_n + \dot{\Phi}(\boldsymbol{x}_n) \end{pmatrix}$$

- The same equation is obtained by using the Jacobi constant $e(t) - \boldsymbol{\Omega} \cdot \boldsymbol{l}(t)$ in steady rotating potentials.
- The potential time-derivative is taken along the trajectory, so can be estimated knowing the particle velocity

$$\begin{aligned} \dot{\Phi}(\boldsymbol{x}(t)) &= \frac{\Phi(\boldsymbol{x}(t+dt)) - \Phi(\boldsymbol{x}(t-dt))}{2dt} + O(dt^2) \\ &\approx \frac{\Phi(\boldsymbol{x}(t) + \boldsymbol{v}(t)dt) - \Phi(\boldsymbol{x}(t) - \boldsymbol{v}(t)dt)}{2dt}, \end{aligned}$$

Jacobi constant 3D method

- The main advantage of Jacobi method in the MW context is to not require spatial gradients, but potential gradients (acceleration and potential time-derivative along the orbit).
- This method is insensitive to extinction but requires some knowledge or further modeling about the total potential.

Moment 3D methods

The moment of inertia tensor ***I***

$$\boldsymbol{I} \equiv \boldsymbol{X}^T \boldsymbol{M} \boldsymbol{X} = \begin{pmatrix} \sum_i m_i x_i^2 & \sum_i m_i x_i y_i & \sum_i m_i x_i z_i \\ \sum_i m_i x_i y_i & \sum_i m_i y_i^2 & \sum_i m_i y_i z_i \\ \sum_i m_i x_i z_i & \sum_i m_i y_i z_i & \sum_i m_i z_i^2 \end{pmatrix}$$

$$\boldsymbol{X} \equiv \begin{pmatrix} x_1 & y_1 & z_1 \\ x_2 & y_2 & z_2 \\ \vdots & \vdots & \vdots \\ x_N & y_N & z_N \end{pmatrix} \qquad \boldsymbol{M} \equiv \begin{pmatrix} m_1 & 0 & \dots & 0 \\ 0 & m_2 & \dots & 0 \\ \vdots & \vdots & \ddots & \vdots \\ 0 & 0 & \dots & m_N \end{pmatrix}$$

can be decomposed in singular values and orthogonal matrices (SVD decomposition)

$$\boldsymbol{I} = USU^T \qquad U = [\boldsymbol{n}_1, \boldsymbol{n}_2, \boldsymbol{n}_3]$$

giving the orthogonal unit directions of the inertia tensor main axes.

Moment 3D methods

Knowing the time derivative of ***I***

$$\dot{\boldsymbol{I}} = \dot{\boldsymbol{X}}^T \boldsymbol{M}\boldsymbol{X} + \boldsymbol{X}^T \boldsymbol{M}\dot{\boldsymbol{X}} = \boldsymbol{V}^T \boldsymbol{M}\boldsymbol{X} + \boldsymbol{X}^T \boldsymbol{M}\boldsymbol{V} = \qquad (1$$

$$\begin{pmatrix} 2\sum_i m_i x_i v_{x_i} & \sum_i m_i(x_i v_{y_i} + y_i v_{x_i}) & \sum_i m_i(x_i v_{z_i} + z_i v_{x_i}) \\ \sum_i m_i(x_i v_{y_i} + y_i v_{x_i}) & 2\sum_i m_i y_i v_{y_i} & \sum_i m_i(y_i v_{z_i} + z_i v_{y_i}) \\ \sum_i m_i(x_i v_{z_i} + z_i v_{x_i}) & \sum_i m_i(y_i v_{z_i} + z_i v_{y_i}) & 2\sum_i m_i z_i v_{z_i} \end{pmatrix}$$

one can obtain by SVD differentiation(*) the exact time differentiation of ***U*** from which the instantaneous rotation vector can be derived

$$\boldsymbol{\Omega} = \boldsymbol{n}_1(t) \wedge \dot{\boldsymbol{n}}_1(t)$$

Any principal vector $\boldsymbol{n}_i$ should give the same result, but the first one, corresponding to the longest principal axis, is numerically more accurate.

(*) algorithm not easily found in the literature

Moment 3D methods

By replacing positions by velocities, and velocities by accelerations, exactly the same ideas can be used for the kinetic tensor,

$$\boldsymbol{K} \equiv \boldsymbol{V}^T \boldsymbol{M} \boldsymbol{V} = \begin{pmatrix} \sum_i m_i v_{x_i}^2 & \sum_i m_i v_{xi} v_{y_i} & \sum_i m_i v_{xi} v_{zi} \\ \sum_i m_i v_{xi} v_{y_i} & \sum_i m_i v_{y_i}^2 & \sum_i m_i v_{y_i} v_{zi} \\ \sum_i m_i v_{xi} v_{zi} & \sum_i m_i v_{y_i} v_{zi} & \sum_i m_i v_{z_i}^2 \end{pmatrix}$$

where rotation occurs now in velocity space.

This method is more sensitive to time perturbation.

Moment 2D methods

If the rotation axis direction is known, one can use the equivalent 2D inertia tensor ***I*** and solve for the pattern speed analytically (without invoking the SVD algorithm):

$$I_{xx} = \sum_i m_i x_i^2, \quad I_{yy} = \sum_i m_i y_i^2, \quad I_{xy} = \sum_i m_i x_i y_i.$$

$$\dot{I}_{xy} = \sum_i m_i \left(x_i v_{y_i} + y_i v_{xi} \right),$$

$$D_{xy} = \frac{1}{2}\left(I_{xx} - I_{yy} \right) = \frac{1}{2} \sum_i m_i \left(x_i^2 - y_i^2 \right),$$

$$\dot{D}_{xy} = \sum_i m_i \left(x_i v_{xi} - y_i v_{y_i} \right),$$

$$\Omega_z \equiv \dot{\phi}(t) = \frac{1}{2} \frac{D_{xy} \dot{I}_{xy} - \dot{D}_{xy} I_{xy}}{D_{xy}^2 + I_{xy}^2}.$$

Fourier 2D method

- For disks of particles one can analyze the Fourier modes *m* in concentric rings where the particle azimuths are $\theta_j = \arctan(y_j, x_j)$

$$F_m = \sum_j m_j \exp(im\theta_j) = \sum_j m_j \left(\cos(m\theta_j) + i\sin(m\theta_j)\right)$$

- The mode phase is a function of positions

$$\phi_m = \arctan(\Im(F_m), \Re(F_m))$$

and can be time-differentiated, giving the instantaneous phase speed, related to the real space speed by

$$\Omega_m \equiv \frac{\dot{\phi}_m}{m} = \frac{1}{m}\,\frac{\dot{\Im}(F_m)\Re(F_m) - \dot{\Re}(F_m)\Im(F_m)}{\Re(F_m)^2 + \Im(F_m)^2}$$

Fourier 2D method

- All the terms are simple sums of trigonometric terms depending on the particle positions and velocities

$$\theta_j = \arctan(y_j, x_j)$$

$$\dot{\theta}_j = \frac{x_j \dot{y}_j - y_j \dot{x}_j}{x_j^2 + y_j^2} = \frac{x_j v_{y\,j} - y_j v_{x\,j}}{x_j^2 + y_j^2}$$

$$C \equiv \sum_j m_j \cos(m\theta_j), \quad S \equiv \sum\nolimits_j m_j \sin(m\theta_j),$$

$$C_1 \equiv \sum_j m_j \cos(m\theta_j)\,\dot{\theta}_j, \; S_1 \equiv \sum\nolimits_j m_j \sin(m\theta_j)\,\dot{\theta}_j$$

$$\Omega_m = \frac{CC_1 + SS_1}{C^2 + S^2}$$

Fourier 2D methods

- Differentiating once more one gets the mode instantaneous pattern acceleration, requiring knowing the particle accelerations,

$$\ddot{\theta}_j = \frac{\left(x_j a_{y\,j} - y_j a_{x\,j}\right) - 2\dot{\theta}_j \left(x_j v_{x\,j} + y_j v_{y\,j}\right)}{x_j^2 + y_j^2}$$

$$C_2 \equiv \sum_j m_j \left[\cos(m\theta_j)\,\ddot{\theta}_j - m\sin(m\theta_j)\,\dot{\theta}_j^2\right]$$

$$S_2 \equiv \sum_j m_j \left[\sin(m\theta_j)\,\ddot{\theta}_j + m\cos(m\theta_j)\,\dot{\theta}_j^2\right]$$

$$\frac{\dot{\Omega}_m}{\Omega_m} = \frac{CC_2 + SS_2}{CC_1 + SS_1} + 2m\frac{CS_1 - SC_1}{C^2 + S^2}$$

Some preliminary results

- We have a couple of new methods to determine the instantaneous and local pattern speed, in 3D or 2D, according to the assumptions made about the pattern.
- The 3D regional Tremaine-Weinberg method works well far from the bar principal axes, but is sensitive to extinction.
- The m=2 Fourier method is less sensitive to perturbations than the 2D moment method.
- The 3D Jacobi method is promising for use in the MW bar, because it requires only a set of individual stars positions and velocities together with a modeled potential.
- In N-body models the Jacobi method shows sensitivity to time-dependence near the centre, because there the long range smooth forces become negligible wrt nearby fluctuating forces.
- The kinematic tensor method is very sensitive to perturbations (cf. the vertex deviation)

Corotation study in double bar N-body models
(Wu, P & Taam 2016)

- 30% of barred galaxies possess a secondary nested bar (Erwin 2011)
- Initial equilibrium axisymmetric conditions with 3 Miyamoto-Nagai (75) models (with GalIC: Yurin & Springel 14)
- $N = 2 \cdot 10^7$ particles, run over 8 Gyr with parallelized gyfalcON (Dehnen 2000).
- Cold inner disk as in Du et al. (15) => Formation of long-lived nested bars + spiral arms

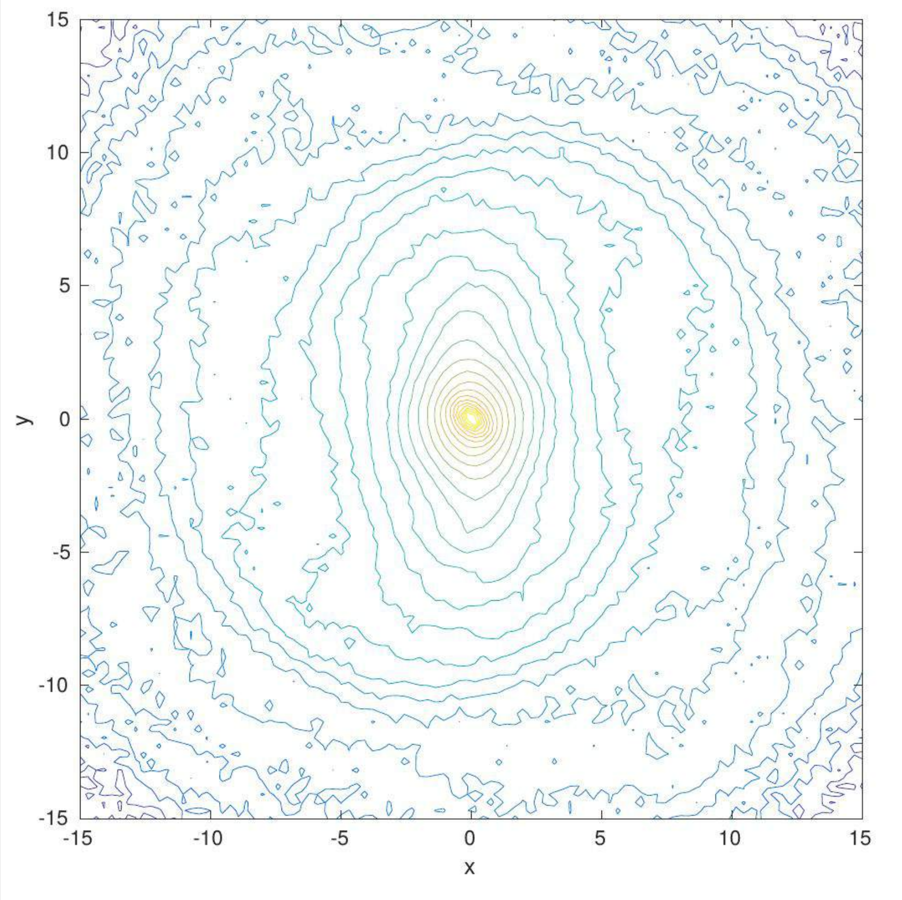

- Inner and outer bars corotation regions study
- How do the equilibrium points behave in the respective rotating frames?

Model

- Miyamoto-Nagai (1975) density components

$$\rho_{MN}(R,z) = \left(\frac{b^2 M_{MN}}{4\pi}\right) \frac{aR^2 + (a + 3\sqrt{z^2+b^2})(a+\sqrt{z^2+b^2})^2}{\left[R^2 + (a+\sqrt{z^2+b^2})^2\right]^{5/2} (z^2+b^2)^{3/2}},$$

Parameter	Halo	Disk	Bulge
Mass M (10^{10} $M_\odot$)	15.0	8.6504	1.3496
Scale length a+b (kpc)	15.0	4.5	0.5
Scale height b (kpc)	15.0	0.45	0.15

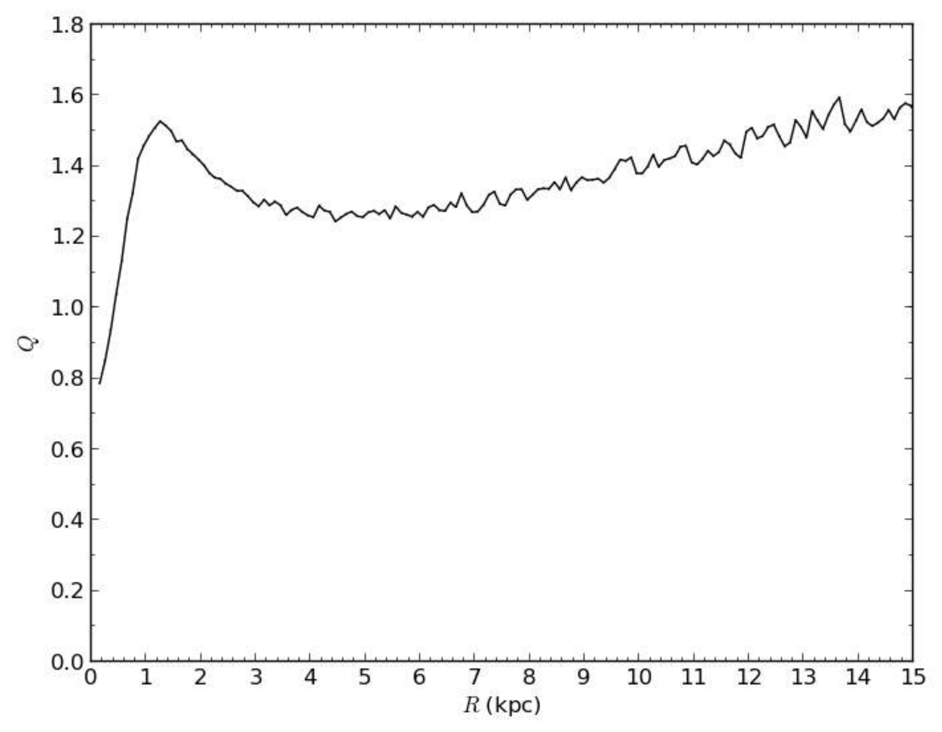

Corotation study in double bar N-body models
(Wu, P & Taam 2016)

- The bar pattern speeds are determined using the 2D moment method
- Instantaneous equilibrium points: extrema of the effective potential,

$$\Phi_{\rm eff} = \Phi - \frac{1}{2}\Omega_{\rm b}^2 R^2$$

- or the location (*x,y*) of the zero acceleration in the respective rotating frames,

$$\begin{aligned}
0 &= a_R + \Omega_{\rm b}^2 R = \frac{a_x x + a_y y}{R} + \Omega_{\rm b}^2 R, \\
0 &= a_\phi = \frac{a_x y - a_y x}{R}, \\
0 &= a_z.
\end{aligned}$$

- or the location in the *x-y* plane with minimum

$$\left(a_x x + a_y y + \Omega_{\rm b}^2 R^2\right)^2 + \left(a_x y - a_y x\right)^2$$

Corotation study in double bar N-body models
(Wu, P & Taam 2016)

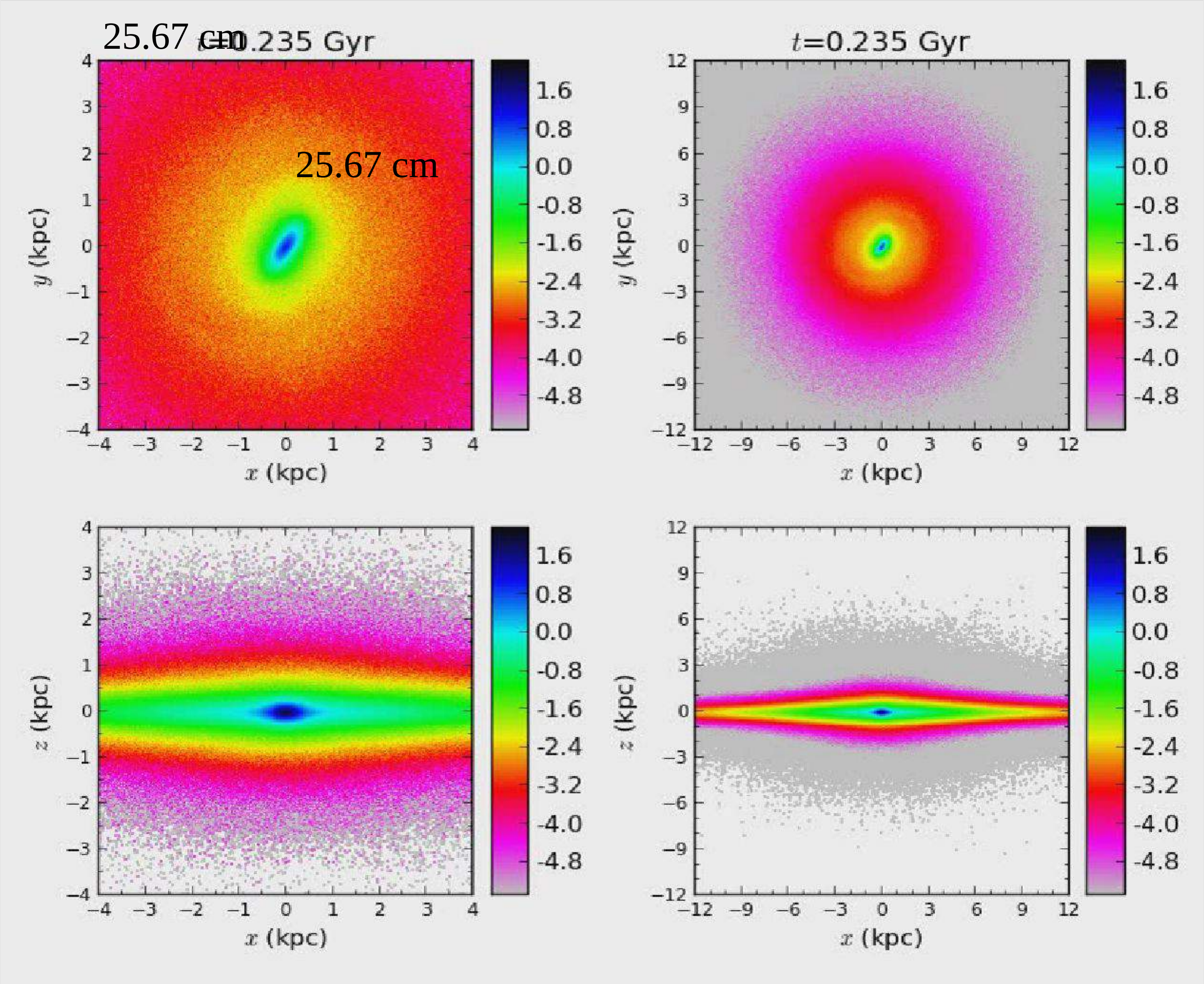

Corotation study in double bar N-body models
(Wu, P & Taam 2016)

- Zero-radial acceleration (black) and zero-torque (white) curves at different times

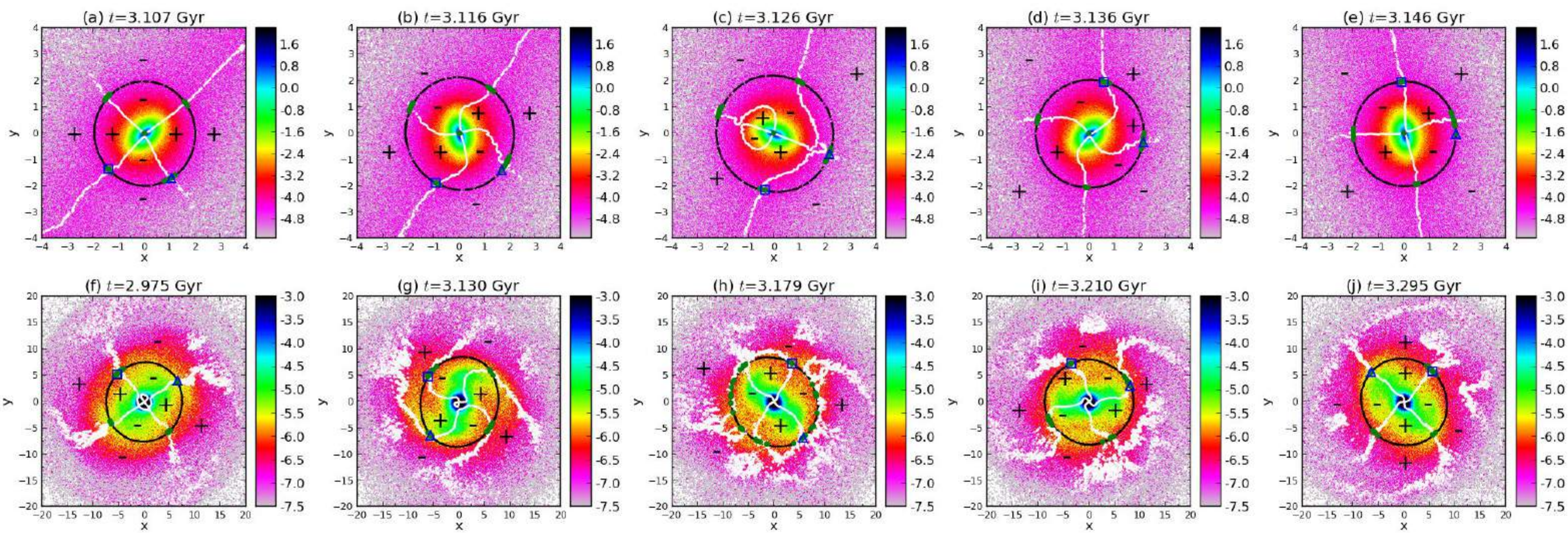

Corotation study in double bar N-body models
(Wu, P & Taam 2016)

- Equilibrium points radii
  (red: inner bar, black: outer bar)

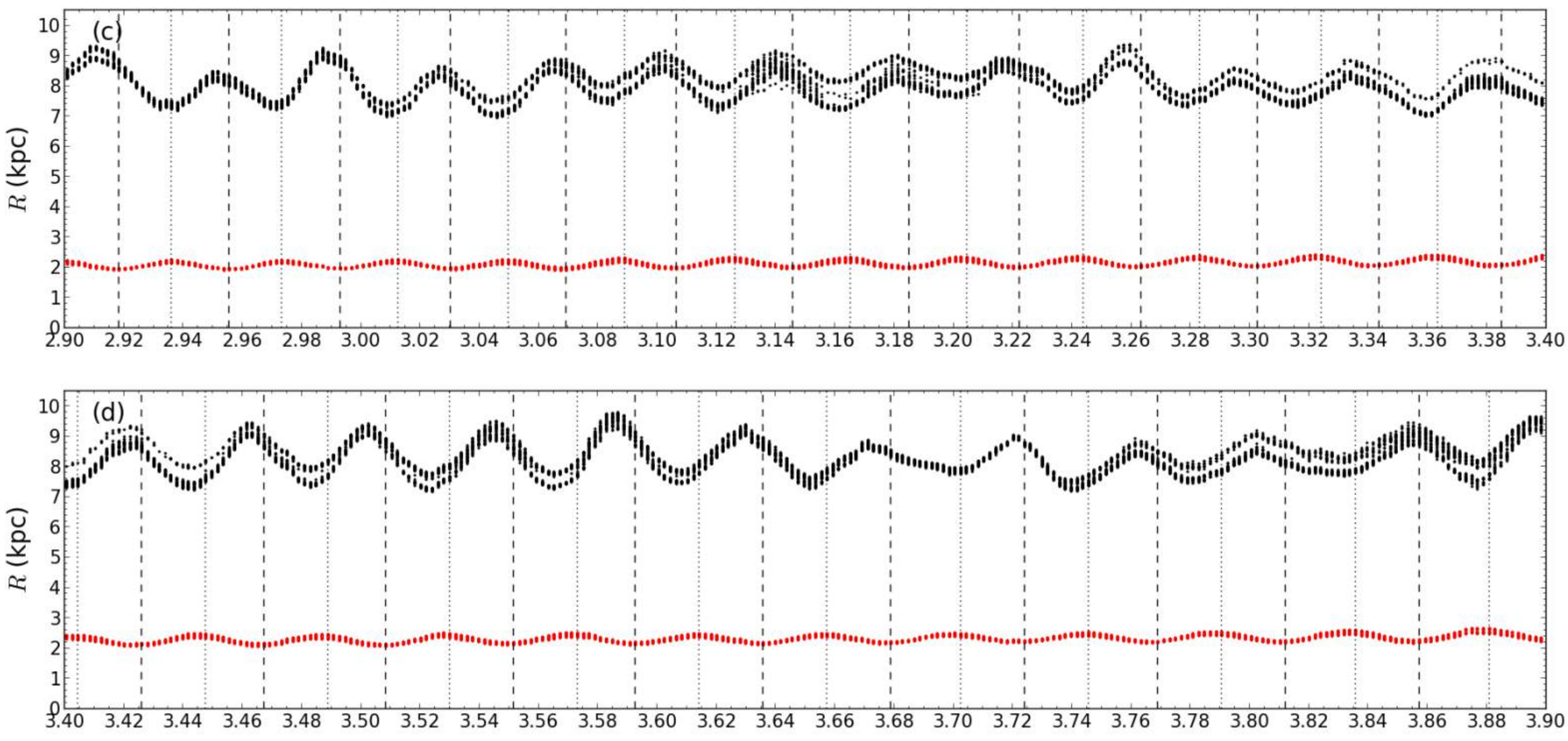

Corotation study in double bar N-body models
(Wu, P & Taam 2016)

- Equilibrium points reduced azimuths (red: inner bar, black: outer bar)

$$\phi_L = \phi_i - \bar{\Omega}_0(t - t_o).$$

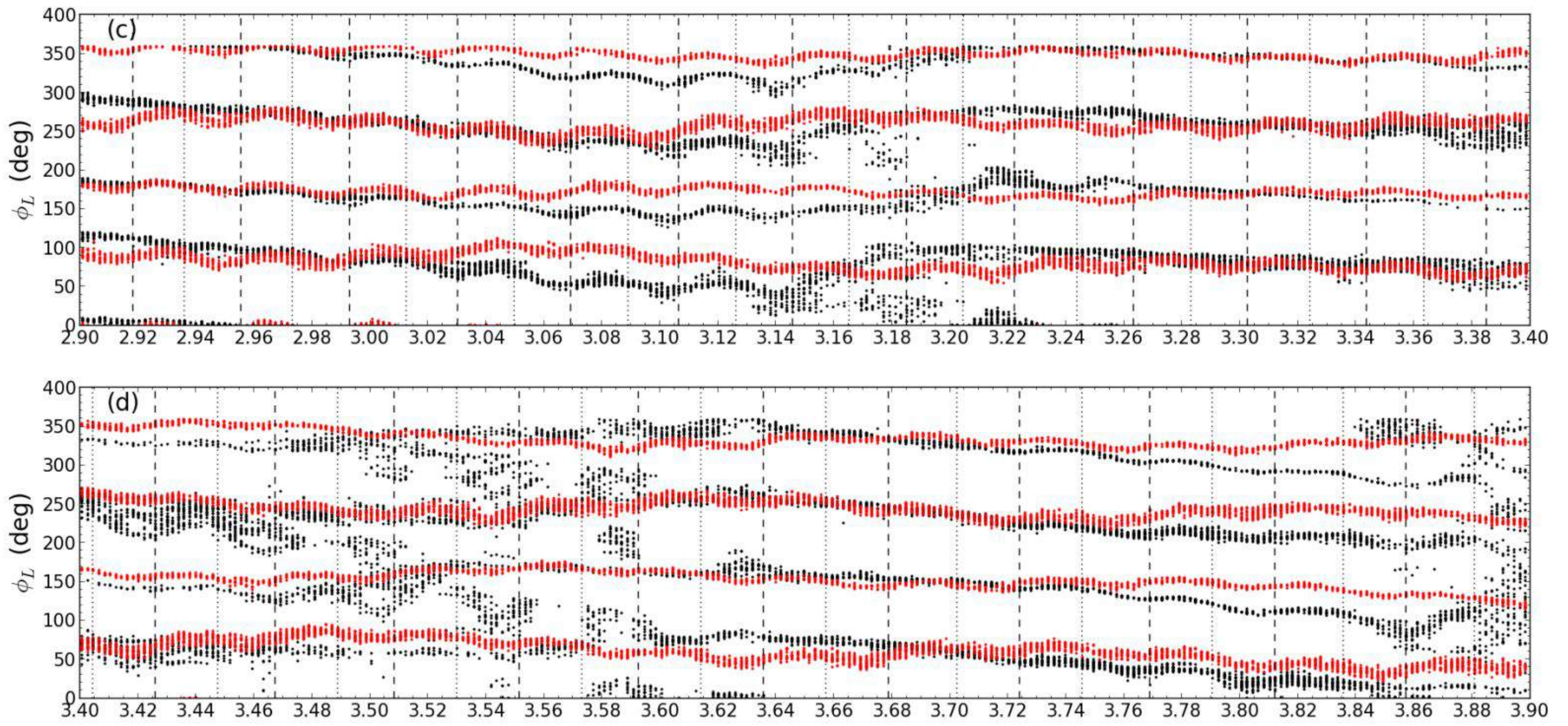

Corotation study in double bar N-body models
(Wu, P & Taam 2016)

- Equilibrium points effective potential
  (red: inner bar, black: outer bar)

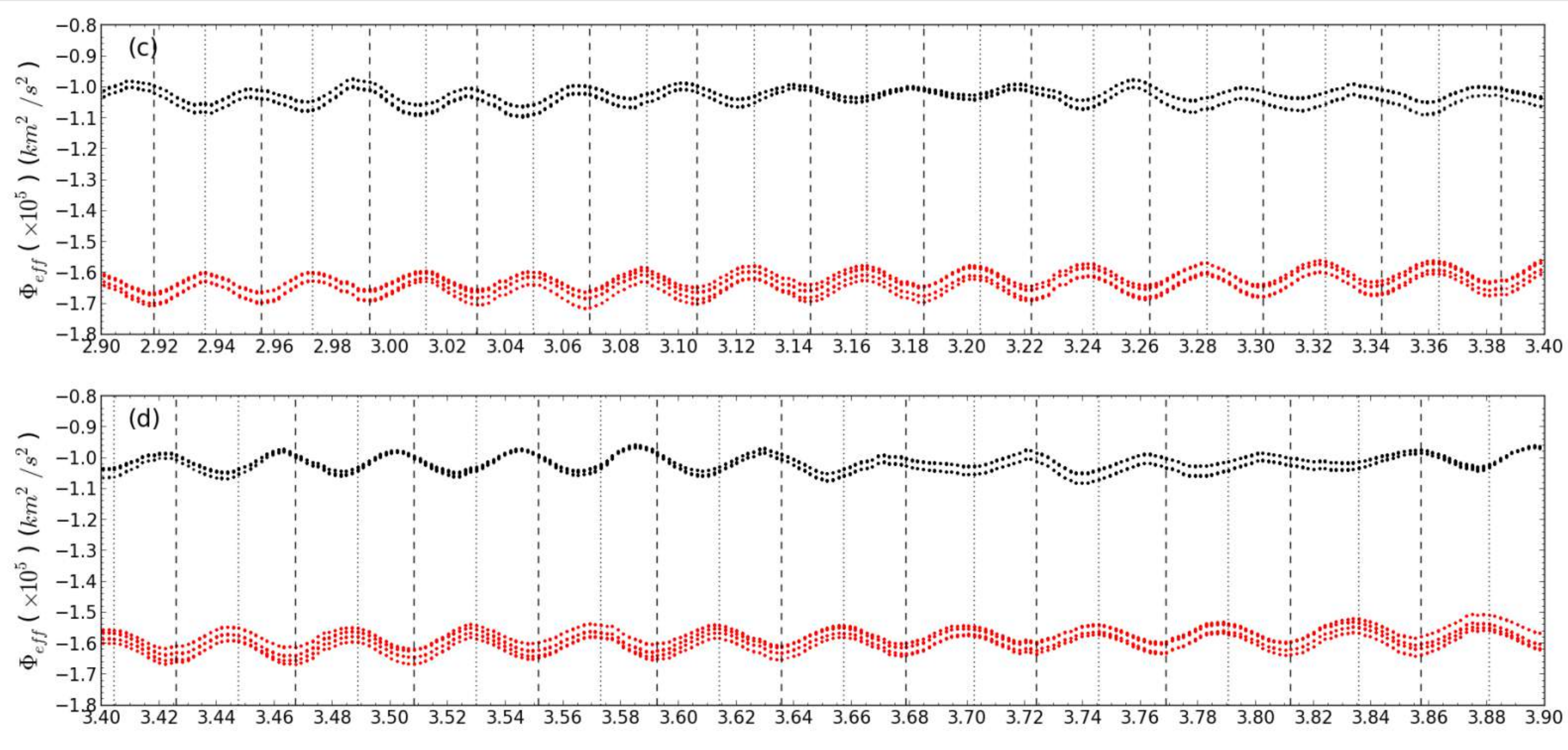

Detailed analysis of the double bar N-body model

(Wu, P & Taam submitted)

Moment of inertia 2D

Radius

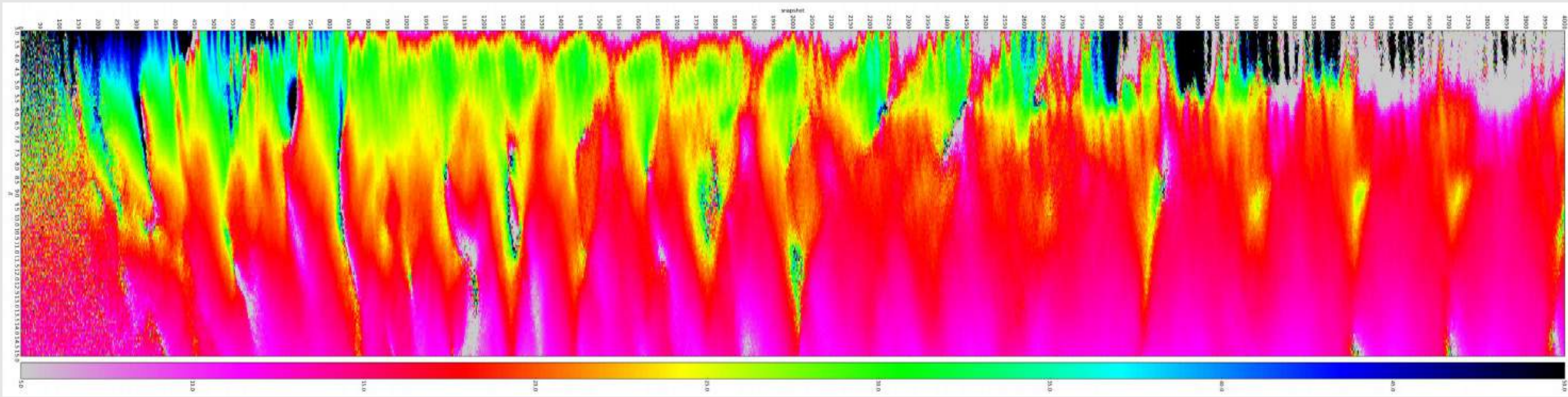

Fourier m=2

Radius

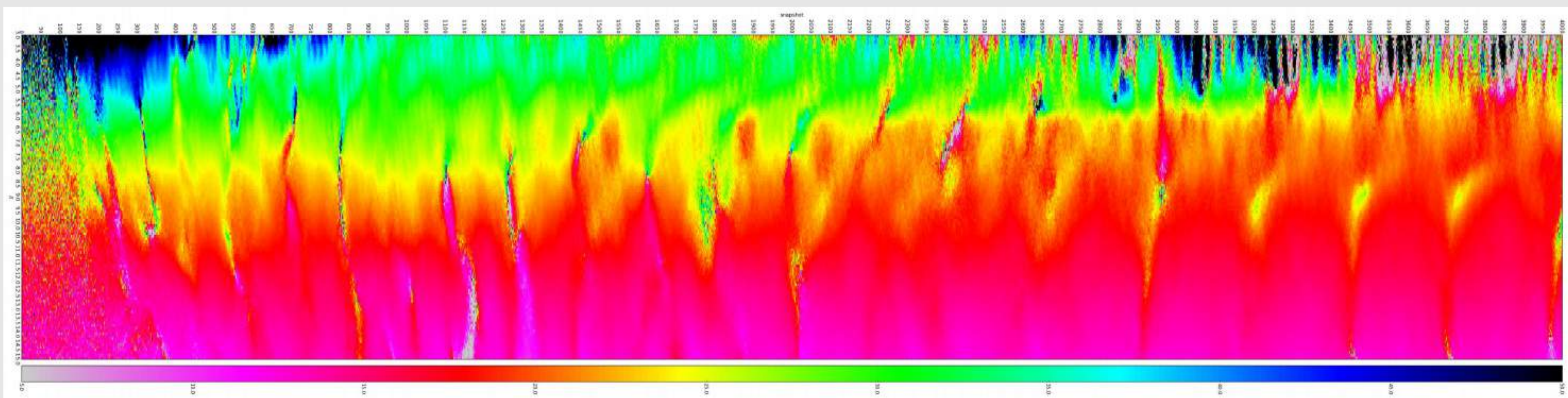

Time

Pattern speed

Time

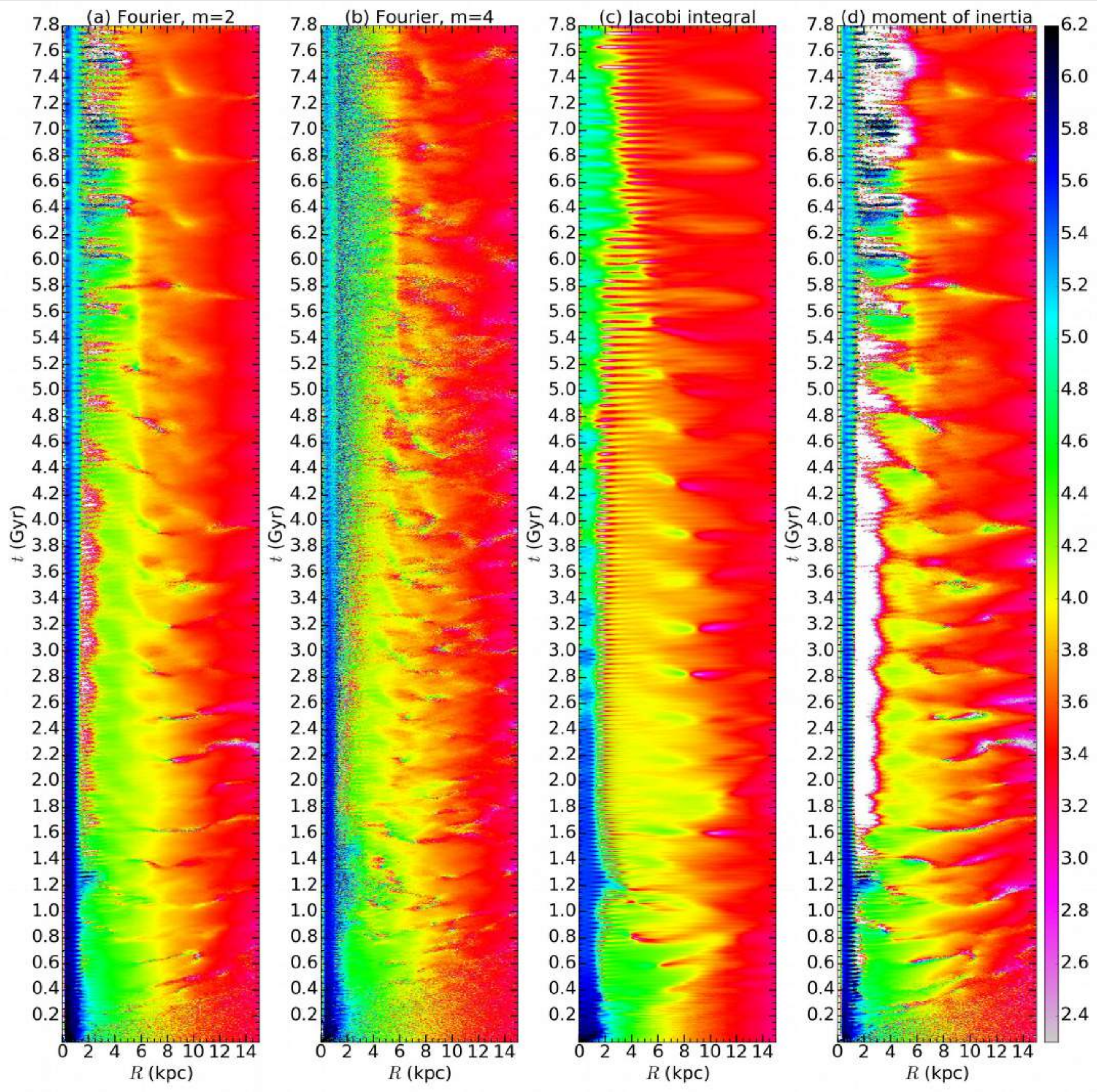

Pattern speed (outer bar)

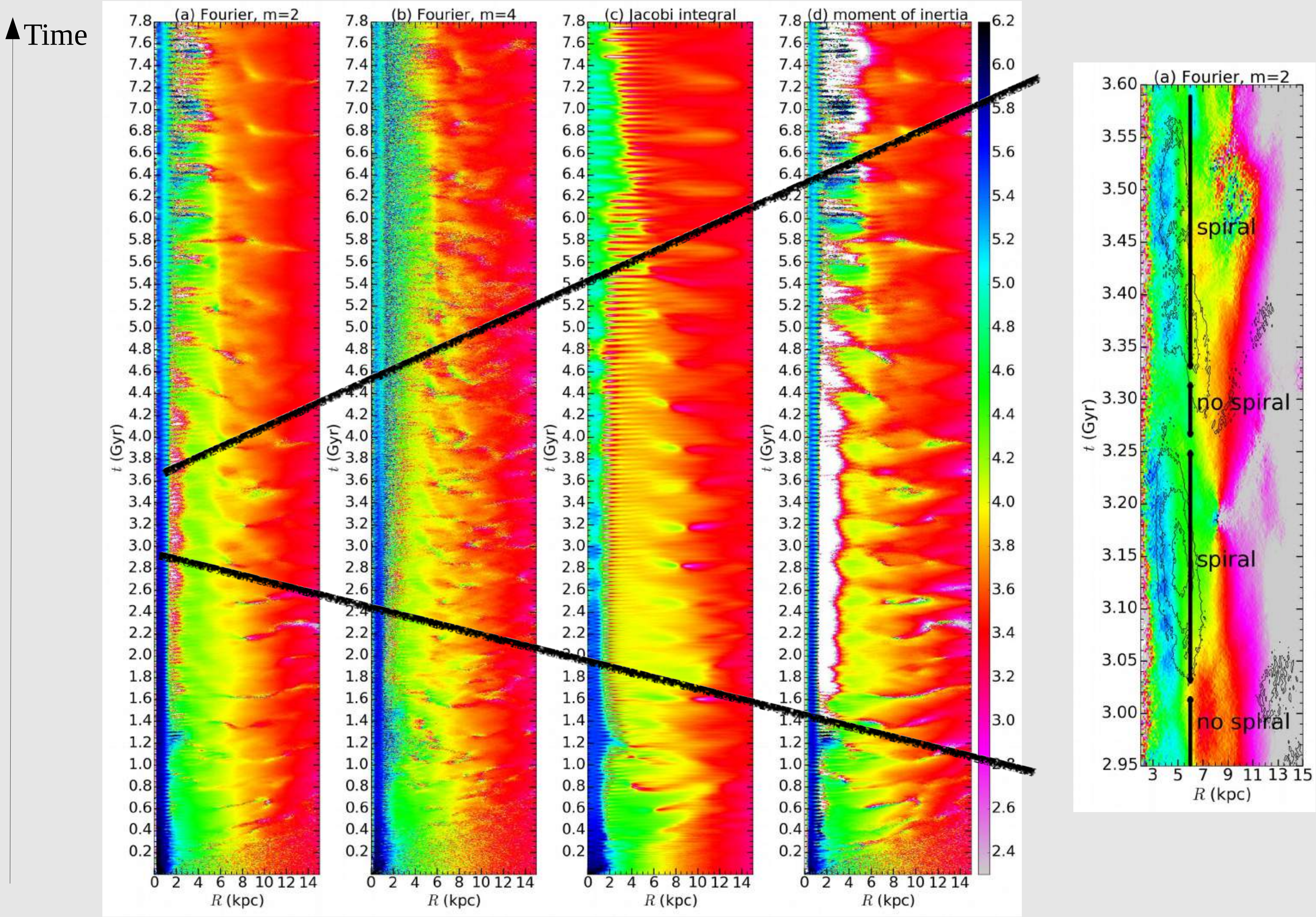

Time

Pattern speed (inner bar)

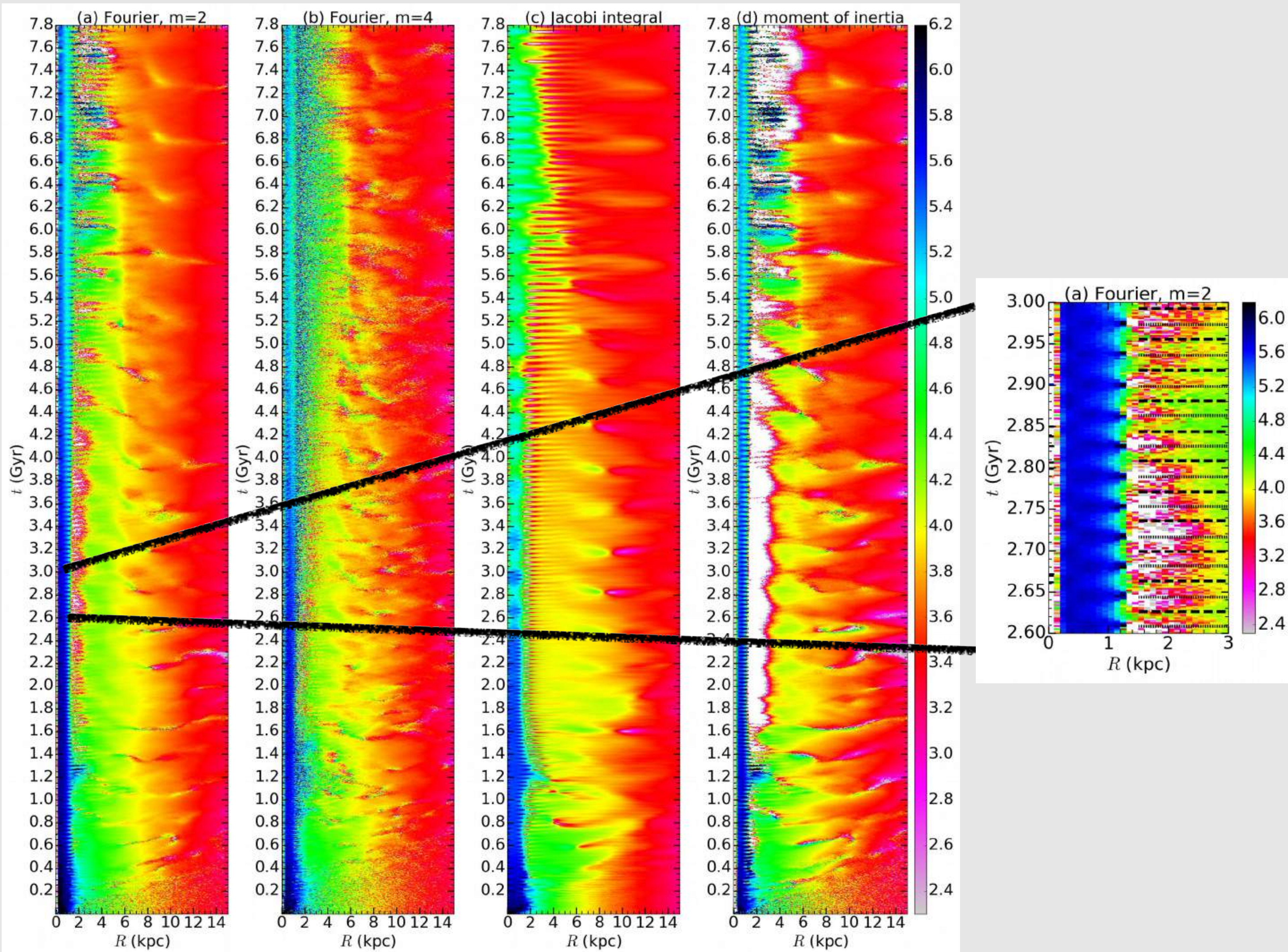

Strength

Time

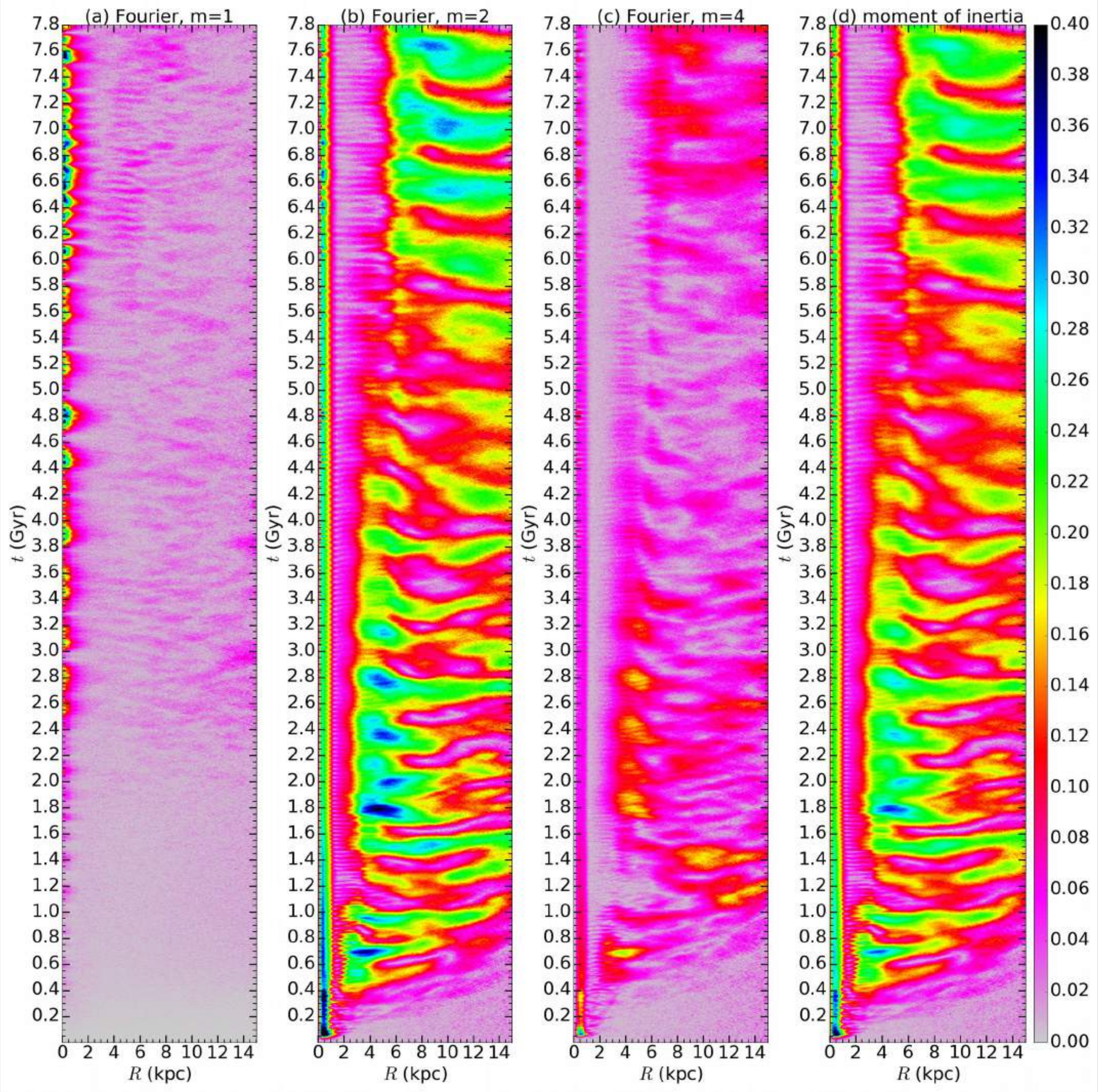

Strength (outer bar)

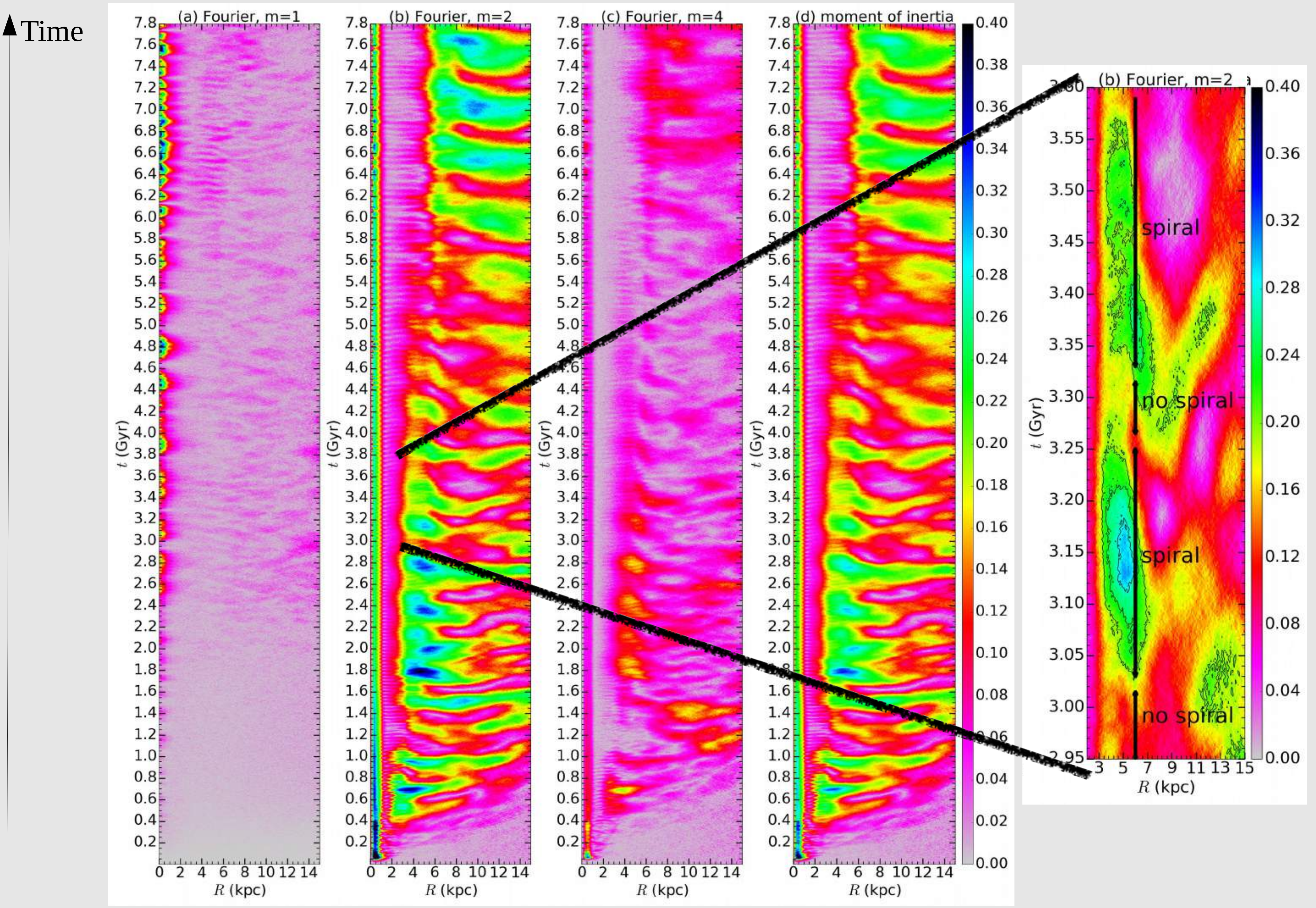

Time

Strength (inner bar)

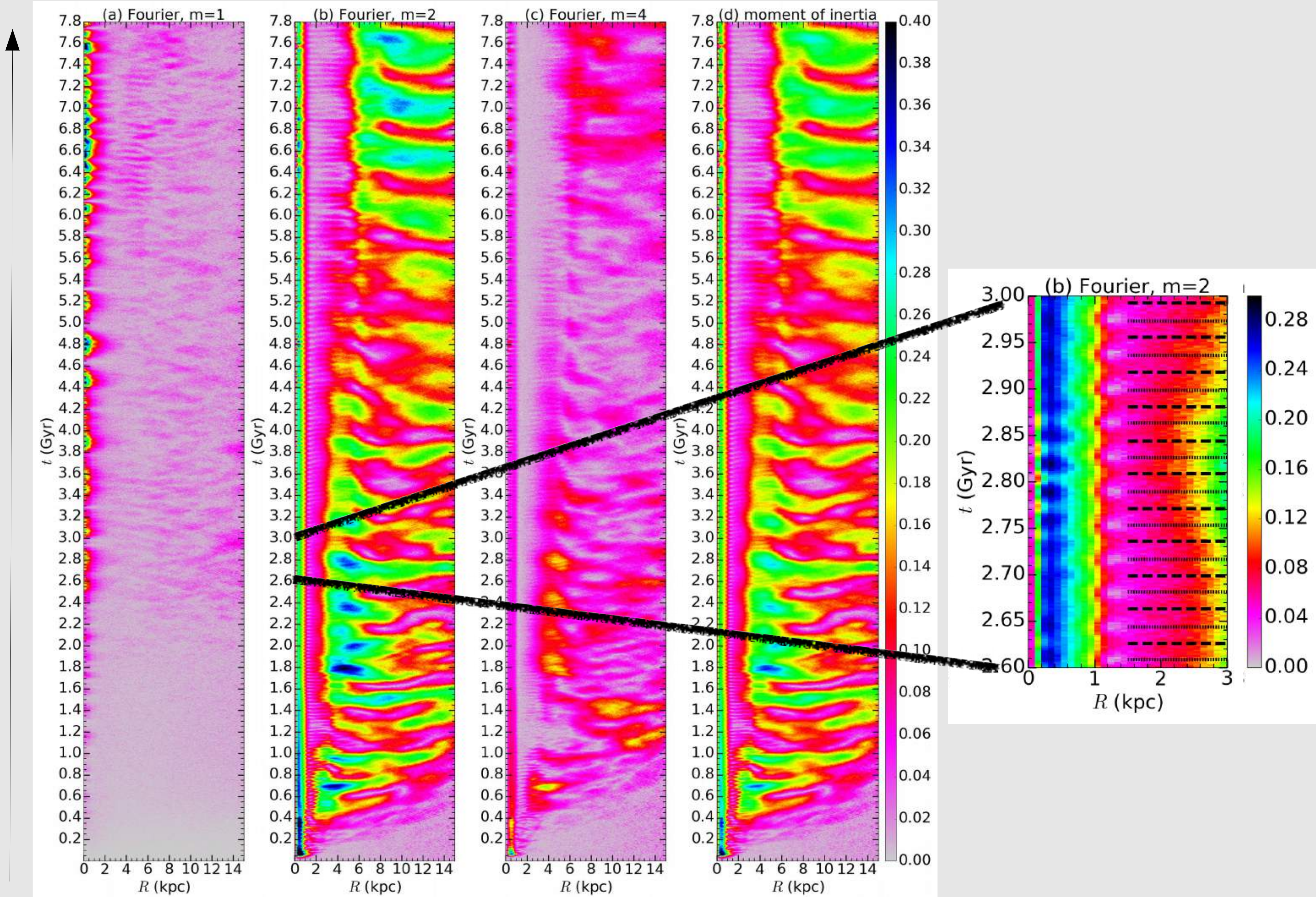

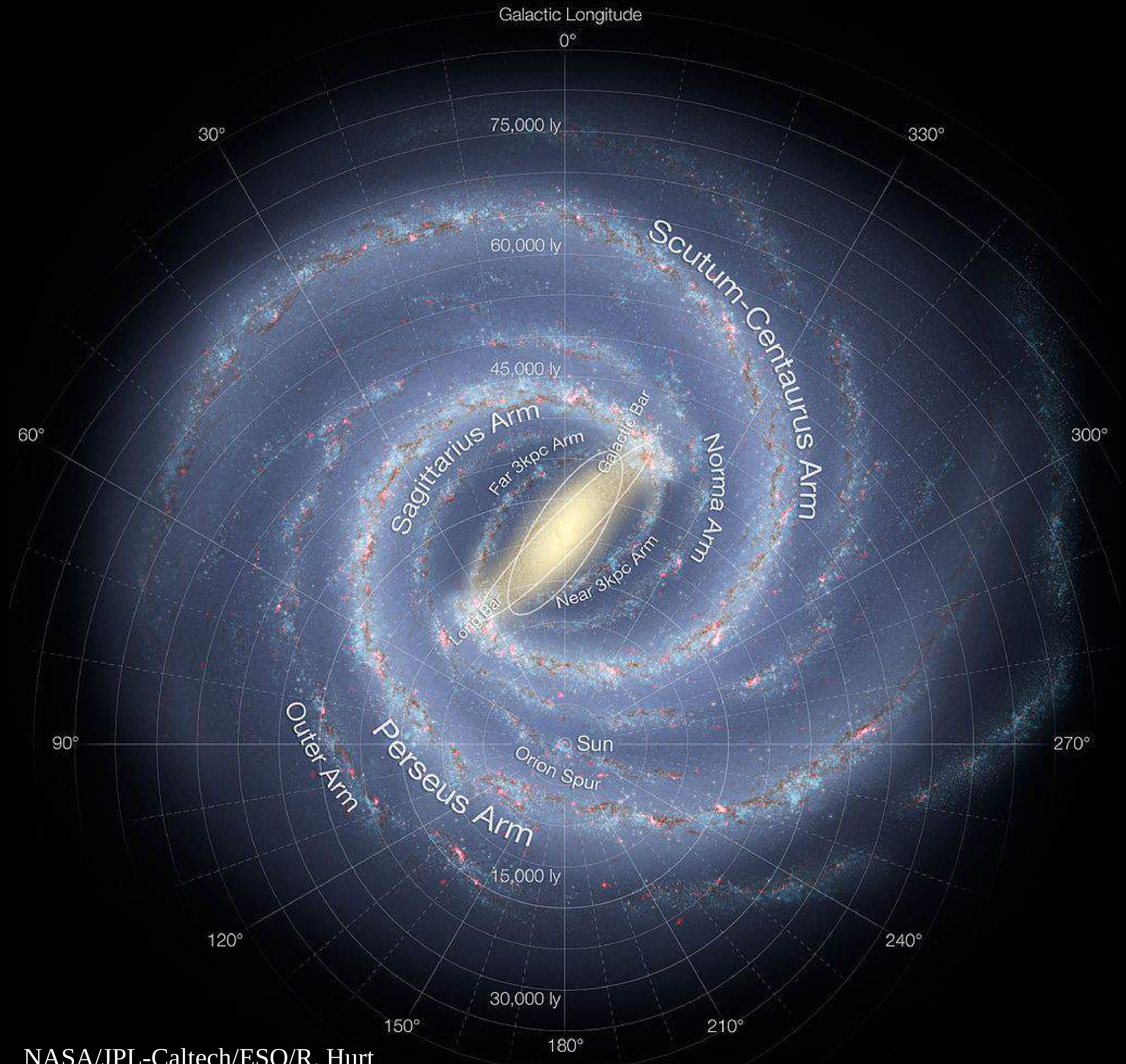

NASA/JPL-Caltech/ESO/R. Hurt

Conclusions

- The corotation regions are particularly time-dependent, the adjacent patterns rotating with different speeds torque each other in time with similar strengths (logical corollary of Sellwood 85)
  - no strict stationary equilibrium points (Lagrange points) exist as well as the Jacobi integral,
  - enhanced chaos, fast stellar diffusion/migration between the bar and the disk, secular evolution
- At any time bars surrounded by spirals are in a particular state of flexion related to the bar/spiral phase difference
  - assuming a rigid bar pattern leads to conflicts about the MW bar pattern speed and orientation in the literature
- The OLR induced by a bar in the spiral region (around the Sun in the MW) should be even more perturbed by local spiral arms than the corotation resonance and can have a meaning only in an time-averaged sense.